

Identification of novel F508del-CFTR traffic correctors among triazole derivatives

Mafalda Bacalhau^a, Filipa C. Ferreira^a, Arthur Kmit^a, Felipe R. Souza^b, Verónica D. da Silva^b, André S. Pimentel^b, Margarida D. Amaral^a, Camilla D. Buarque^{b,1}, Miquéias Lopes-Pacheco^{a,*,1}

^a Biosystems & Integrative Sciences Institute (BioISI), Faculty of Sciences, University of Lisbon, Lisbon, Portugal

^b Department of Chemistry, Pontifical Catholic University of Rio de Janeiro (PUC-Rio), Rio de Janeiro, Brazil

ARTICLE INFO

Keywords:

CFTR modulator
Cystic fibrosis
Drug discovery
Genetic revertants
Intracellular trafficking
Low temperature
Protein folding

ABSTRACT

The most prevalent cystic fibrosis (CF)-causing mutation – F508del – impairs the folding of CFTR protein, resulting in its defective trafficking and premature degradation. Small molecules termed correctors may rescue F508del-CFTR and therefore constitute promising pharmacotherapies acting on the fundamental cause of the disease. Here, we screened a collection of triazole compounds to identify novel F508del-CFTR correctors. The functional primary screen identified four hit compounds (LSO-18, LSO-24, LSO-28, and LSO-39), which were further validated and demonstrated to rescue F508del-CFTR processing, plasma membrane trafficking, and function. To interrogate their mechanism of action (MoA), we examined their additivity to the clinically approved drugs VX-661 and VX-445, low temperature, and genetic revertants of F508del-CFTR. Rescue of F508del-CFTR processing and function by LSO-18, LSO-24, and LSO-28, but not by LSO-39, was additive to VX-661, whereas LSO-28 and LSO-39, but not LSO-18 nor LSO-24, were additive to VX-445. All compounds under investigation demonstrated additive rescue of F508del-CFTR processing and function to low temperature as well as to rescue by genetic revertants G550E and 4RK. Nevertheless, none of these compounds was able to rescue processing nor function of DD/AA-CFTR, and LSO-39 (similarly to VX-661) exhibited no additivity to genetic revertant R1070W. From these findings, we suggest that LSO-39 (like VX-661) has a putative binding site at the NBD1:ICL4 interface, LSO-18 and LSO-24 seem to share the MoA with VX-445, and LSO-28 appears to act by a different MoA. Altogether, these findings represent an encouraging starting point to further exploit this chemical series for the development of novel CFTR correctors.

1. Introduction

Cystic fibrosis (CF), the most common lethal autosomal recessive disease among Caucasians, is caused by mutations in the gene encoding the CF transmembrane conductance regulator (CFTR) protein, a cAMP-regulated Cl[−]/HCO₃[−] channel located at the apical plasma membrane (PM) of several epithelia (Lopes-Pacheco, 2020; Pinto et al., 2021; Riordan et al., 1989). In the respiratory tract, CFTR dysfunction causes abnormal ion transport and dehydration of airway surface liquid that leads to mucociliary clearance impairment. As a consequence, individuals with CF face recurrent respiratory infections and chronic inflammation that ultimately results in end-stage lung disease (Lopes-Pacheco, 2020; Pinto et al., 2021).

The deletion of a phenylalanine residue at position 508 (F508del) is

the most prevalent CF-causing mutation, occurring in 80–85% of CF cases worldwide (Lopes-Pacheco, 2020). The F508del-CFTR protein is unstable and incorrectly folded, being thus retained by endoplasmic reticulum quality control (ERQC), which rapidly targets it to degradation via the ubiquitin-proteasome system (Jensen et al., 1995; Kim and Skach, 2012; Lopes-Pacheco et al., 2015). Nevertheless, several studies demonstrated that F508del-CFTR traffic can be partially rescued by low-temperature incubation of cells expressing this mutant (Denning et al., 1992; Sharma et al., 2001; Wang et al., 2008). Several second-site revertant mutations that are *in cis* with F508del were also demonstrated to rescue F508del-CFTR by distinct mechanisms of action (MoA's) (Chang et al., 1999; Decarvalho et al., 2002; Farinha et al., 2013; Lopes-Pacheco et al., 2022; Prins et al., 2022; Rabeh et al., 2012; Roxo-Rosa et al., 2006; Thibodeau et al., 2010).

Following experimental evidence that F508del-CFTR is rescuable,

* Corresponding author.

E-mail address: mlpacheco@fc.ul.pt (M. Lopes-Pacheco).

¹ These authors share senior authorship.

Abbreviations:

ADME	absorption, distribution, metabolism and excretion
AFT	arginine framed tripeptide
ATP	adenosine triphosphate
cAMP	cyclic adenosine monophosphate
CF	cystic fibrosis
CFBE	CF bronchial epithelial
CFTR	CF transmembrane conductance regulator
DMEM	Dulbecco's modified Eagle medium
DMSO	dimethyl sulfoxide
EMEM	Eagle's minimum essential medium
ER	endoplasmic reticulum
ERQC	ER quality control
FBS	fetal bovine serum
Fsk	forskolin
FRT	Fischer rat thyroid
Gen	genistein
HEK	human embryonic kidney
HS-YFP	halide sensitive-yellow fluorescence protein

ICL	intracellular loop
LogP	calculated logarithm of the octanol-water partition coefficient
MoA	mechanism of action
MW	molecular weight
NBD	nucleotide binding domain
nHBA	number of H-bond acceptors
nHBD	number of H-bond donors
nRB	number of rotatable bonds
PAINS	pan-assay interference structures
PBS	phosphate-buffered solution
PDB	protein database
PM	plasma membrane
PVDF	polyvinylidene difluoride
R _{te}	transepithelial resistance
TMD	transmembrane domain
TPSA	topological polar surface area
V _{te}	transepithelial voltage
WB	Western blot
WT	wild type

high-throughput assays have been developed to screen small molecule libraries and thus identify compounds capable of correcting the folding defect and restoring traffic of this protein to the PM (Lopes-Pacheco et al., 2021; Pedemonte et al., 2005; Van Goor et al., 2006). However, only recently a 'highly effective' triple combo drug – composed of two correctors (VX-661 and VX-445) to rescue F508del-CFTR traffic plus a potentiator (VX-770) to restore channel gating – was approved for individuals with CF carrying F508del in at least one allele (Middleton et al., 2019; Sutharsan et al., 2022). Despite such accomplishments, this triple combo drug promotes only a partial rescue of F508del-CFTR traffic and function (Capurro et al., 2021; Veit et al., 2020). Meanwhile, several other investigational compounds from various chemical series have been demonstrated to correct F508del-CFTR defects at distinct efficacy levels (Farinha et al., 2013; Lopes-Pacheco et al., 2020, 2022; Pedemonte et al., 2005; Van Goor et al., 2006; Veit et al., 2018).

Triazoles are 5-membered synthetic heterocycle compounds broadly used in the design of novel drugs and proved to be a successful strategy in medicinal chemistry due to their pharmacological versatility and synthetic practicality (Bonandi et al., 2017; Wang et al., 2016). Here, we investigated the ability of a collection of novel triazole compounds in rescuing F508del-CFTR traffic. We initially performed a screen of these compounds using a functional assay in CF bronchial epithelial (CFBE) cells stably expressing F508del-CFTR. After validation by biochemical, immunofluorescence, and functional experiments, the MoA of the four most promising compounds was investigated by assessing their additivity to previously characterized CFTR genetic revertants, which rescue F508del-CFTR by distinct mechanisms: G550E and R1070W restore two different protein structural pockets resulting from the absence of F508del residue (Decarvalho et al., 2002; Lopes-Pacheco et al., 2022; Prins et al., 2022; Rabeh et al., 2012; Roxo-Rosa et al., 2006; Thibodeau et al., 2010), while 4RK affects trafficking by simultaneously removing four arginine framed tripeptide (AFT) retention motifs (R29K/R516K/R555K/R766K) (Chang et al., 1999; Farinha et al., 2013; Lopes-Pacheco et al., 2020; Roxo-Rosa et al., 2006). We also assessed the effects of these compounds on DD/AA-CFTR variant that lacks the double diacidic code (D565A/D567A) (Farinha et al., 2013; Roy et al., 2010; Wang et al., 2004), which abrogates protein trafficking without affecting folding. To gain further understanding of the MoA of these compounds, we also examined their additive effects to the clinically approved correctors VX-661 and VX-445, as well as to low temperature. Finally, we assessed the efficacy of the hit compounds in rescuing other CF-causing mutations.

2. Material and methods

2.1. Cell culture

CFBE cells stably expressing CFTR variants (wild-type [WT], F508del, G85E, L206W, R334W, I507del, R560S, N1303K and DD/AA or carrying G550E, R1070W and 4RK *in cis* with F508del) were cultured in Eagle's minimum essential medium (EMEM, #BE12-611F, Lonza) supplemented with 10% fetal bovine serum (FBS, #10270106, Gibco) and 2 µg/mL puromycin (#P8833, Sigma-Aldrich) (Bebok et al., 2005; Lopes-Pacheco et al., 2022). CFBE cells stably expressing mCherry-Flag-F508del-CFTR under the control of a Tet-On promoter were cultured in Dulbecco's modified Eagle medium (DMEM, #BE12-604F, Lonza) supplemented with 10% FBS, 10 µg/mL blasticidin (#ant-bl, InvivoGen) and 2 µg/mL puromycin (Botelho et al., 2015; Lopes-Pacheco et al., 2020). All cells were maintained in a humidified incubator at 37 °C and 5% CO₂, with an exception for low-temperature experiments in which cells were kept at 27 °C for 48 h.

2.2. Generation of novel cell lines expressing the HS-YFP

CFBE cells stably expressing CFTR variants (F508del, DD/AA, F508del/G550E, F508del/R1070W, and F508del/4RK) were used to generate novel cell lines co-expressing the halide-sensitive yellow fluorescent protein (HS-YFP F46L/H148Q/I152L). The HS-YFP cDNA cloned into the pcDNA3.1 expression vector was re-cloned into the lentiviral expression vector pLVX-Puro by homologous recombination using the In-Fusion HD Cloning Kit (#639649, Clontech-Takara). First, the construct was amplified from the original expression vector by PCR using KOD Hot Start Polymerase (#71086–3, Millipore, Novagen®) and a set of primers (Forward: 5'-GGACTCAGATCTCGAATGGTGAGCAAGGGCGAGGA-3' and Reverse: 5'-GAAGCTTGAGCTCGATTACTTGTACAGCTCGTCCATGC-3') according to the manufacturer's instructions. Then, the pLVX-Puro vector was linearized using a mixture of 20 µL containing 20 U *XhoI* enzyme, 1 × Buffer R, and pLVX-Puro (2 µg), incubated at 37 °C for 3 h followed by 20 min at 80 °C. Second, the linearized pLVX-Puro vector and construct were purified using the NzyGelpure kit (#MBO1101, Nzytech) according to the manufacturer's instructions. After purification, homologous recombination was performed using In-Fusion HD Cloning Kit, using linearized plasmid (75 ng) and construct (100 ng). After incubation at 50 °C for 15 min, the YFP-pLVX-Puro construct was transformed into

competent bacteria and the insertion was verified by sequencing. Plasmid (YFP-pLVX-Puro) was used to calcium phosphate-transfect HEK-293T cells for the production of lentiviral particles. Briefly, the transfection reaction mixture included YFP-pLVX-Puro (2.38 µg), psPAX2 lentiviral packaging plasmid (2.38 µg) (#12260, Addgene), pMD2.G lentiviral packaging plasmid (0.24 µg) (#12259, Addgene) and was performed using the Lipofectamine™ 3000 Transfection Reagent (#L30000015, Invitrogen) and Opti-MEM™, Reduced Serum Medium (#31985047, Gibco), according to the manufacturer's instructions. Cells were incubated for 24 h at 37 °C in 5% CO₂ before replacing the medium and lentiviral particles were collected 48 h after transfection. In order to concentrate the lentiviral particles, PEG-it™ Virus Precipitation Solution (#LV810A-1, System Biosciences) was used according to the manufacturer's instructions. Finally, lentiviral particles were used to transduce CFBE cells stably expressing CFTR variants. An infection mixture containing the collected supernatant with lentiviral particles and EMEM supplemented with 10% FBS and 8 µg/mL of hexadimethrine bromide (polybrene) (#107689-10G, Sigma-Aldrich) was added to CFBE cells seeded on a plate. The plate was centrifuged at 220 rpm for 1 h at 25 °C and placed back in the incubator. The efficiency of the transduction was assessed by fluorescence microscopy (Zeiss Axiovert 200) and then cells were sorted in a FACSaria III cell sorter (BD Biosciences) to select the ones with the highest expression of the HS-YFP.

2.3. Chemicals and compounds

The 1,2,3-triazole-1,4-disubstituted compounds and derivatives were synthesized and structurally characterized as previously described (da Silva et al., 2020, 2019). Compounds were diluted in dimethyl sulfoxide (DMSO) and added to cells diluted in 1% FBS-supplemented antibiotic-free medium. All remaining reagents were purchased from commercial sources at the highest purity available and were also diluted in DMSO: VX-661 (#S7058, Selleckchem), VX-445 (#S8851, Selleckchem), forskolin (Fsk, #66575-29-9, Sigma-Aldrich), genistein (Gen, #446-72-0, Sigma-Aldrich) and CFTR channel inhibitor (CFTRinh-172, #307510-92-5, Sigma-Aldrich). The final concentration of each compound has been indicated in figure legends.

2.4. Measurement of the HS-YFP fluorescence quenching

Determination of CFTR function was performed in CFBE cells stably co-expressing CFTR variants and the HS-YFP (F46L/H148Q/I152L) as previously described (Pedemonte et al., 2010; Sondo et al., 2011). Briefly, after incubation with compounds for 24 h, cells were washed with phosphate-buffered saline (PBS) and then incubated for 30 min with 60 µL of PBS containing Fsk (20 µM) and Gen (50 µM) to maximally stimulate CFTR activity. Cells were then transferred to a microplate reader (Tecan Infinite 200 Pro) equipped with high-quality excitation (485 ± 20 nm) and emission (535 ± 25 nm) filters for YFP. The fluorescence was recorded for 2 s before and 12 s after injection of 165 µL of an I⁻-containing solution (PBS with Cl⁻ replaced by I⁻, final I⁻ concentration: 100 mM). Data were normalized to the initial background-subtracted fluorescence. To determine I⁻ influx rate, the final 11 s of the data for each well were fitted with an exponential function to extrapolate the initial slope (dF/dt). All conditions were performed in triplicate on each plate.

2.5. In silico analysis of absorption, distribution, metabolism, and excretion (ADME)

In silico ADME analysis was performed using the free online software SwissADME (<http://www.swissadme.ch/index.php>) as described (Daina et al., 2017).

2.6. Western blot

Cells were lysed using a lysis buffer (31.25 mM Tris-HCl pH 6.8, 1.5% SDS [w/v], 5% glycerol and 0.5 mM DTT) supplemented with complete protease inhibitor cocktail (#11836153001, Roche) and Laemmli sample buffer (#1610747, Bio-Rad). Protein extracts were separated on 10% gels (w/v), transferred to polyvinylidene difluoride (PVDF) membranes (#88518, Thermo Scientific), and analyzed by Western blot (WB). Membranes were blocked with 3% non-fat milk in tris-buffered saline with 1% tween-20 (#42120501, Biolife Italiana) and probed with the monoclonal anti-human CFTR antibody 596 (1:3000; CF Foundation Therapeutics) or with the monoclonal anti-calnexin antibody (1:3000; BD Biosciences, used as a loading control) diluted in blocking buffer. Membranes were washed and incubated with the blotting-grade horseradish peroxidase secondary antibody (1:3,000, #170-6516, Bio-Rad) also diluted in blocking buffer. Chemiluminescent detection was performed using the Clarity Western ECL substrate (#1705061, Bio-Rad) and the Chemidoc XRS system. Band intensity was quantified using the Image Lab software (version 6.0, Bio-Rad) and normalized to the loading control as appropriate.

2.7. Immunostaining and fluorescence microscopy

The traffic assay was carried out as previously described (Botelho et al., 2015). Briefly, 24 h after seeding CFBE cells expressing the inducible mCherry-Flag-F508del-CFTR traffic report onto clear-bottom 384-well black plates, CFTR expression was induced by adding 1 µg/mL doxycycline (#9891, Sigma-Aldrich) to the culture medium, and 24 h later, compounds were administered. After the 72 h assay time, cells underwent an immunofluorescence protocol to detect extracellular Flag tags without cell permeabilization (Botelho et al., 2015; Lopes-Pacheco et al., 2022). Briefly, cells were incubated for 1 h with an anti-Flag M2 monoclonal antibody (1:500, #F1804, Sigma-Aldrich), fixed with 3% paraformaldehyde, and then incubated for 1 h with an anti-mouse Alexa Fluor® 647 conjugated secondary antibody (1:500, #A31571, Molecular Probes). The nuclei were counterstained with a Hoechst 33,342 solution (1:5,000, #S2261, Sigma-Aldrich) and used for contrast-based autofocus. Cell imaging was performed in an inverted epifluorescence microscope Leica DMI6000 (Leica Microsystems). Automatic image analysis was performed with CellProfiler using a pipeline developed to measure CFTR traffic efficiency also as described (Botelho et al., 2015). The background was first subtracted from each image to correct the illumination and background fluorescence. Thereafter, quality control was applied to exclude cells that do not express CFTR, have aberrant morphology, or have a considerable number of saturated pixels. Finally, the mCherry tags were used to quantify the total amount of CFTR protein expressed by each cell, while the stained Flag tags allowed for the quantification of CFTR located exclusively at the PM. All conditions were performed in triplicate on each plate.

2.8. Micro-ussing chamber measurements

CFBE cells stably expressing F508del-CFTR were grown onto Snapwell inserts (#734-1646, Corning-Costar, USA) to establish polarized monolayers. The transepithelial electrical resistance of cells was measured with the Chopstick Electrode (STX2, WPI), and when it was ≥1000 Ω·cm², cells were incubated with compounds for 24 h. Subsequently, recordings were performed in modified micro-Ussing chambers. Briefly, the basolateral surface of CFBE cells expressing F508del-CFTR was continuously perfused with Ringer solution (in mM: 145 NaCl, 1.6 K₂HPO₄, 5.0 D-glucose, 1.0 MgCl₂, 1.3 Ca-gluconate) and the apical surface with a low Cl⁻ Ringer solution (in mM: 32 NaCl, 0.4 KH₂PO₄, 1.6 K₂HPO₄, 5.0 D-glucose, 1.0 MgCl₂, 5.7 Ca-gluconate and 112 Na-glucose). Baseline values were recorded after the equilibration period, and Fsk (2 µM), Gen (50 µM), and CFTRinh-172 (30 µM) were added sequentially. Transepithelial resistance (R_{te}) and the voltage (V_{te})

were recorded, and equivalent cAMP-stimulated CFTR short-circuit currents (ΔI_{eq-sc}) were calculated by Ohm's law from V_{te} and R_{te} ($I_{eq-sc} = V_{te}/R_{te}$).

2.9. Molecular docking

Molecular modeling methods were applied to evaluate the potential binding sites of the compounds under investigation. Two three-dimensional structures were obtained from the protein data bank (PDB) (Berman et al., 2000) to study the NBD1:ICL4 site and the potential binding sites in the NBD1 domain. To evaluate the NBD1:ICL4 site, the complete three-dimensional structure of the CFTR, PDB code 6O2P (Liu et al., 2019), with a spherical constraint with a radius of 11 Å, centered on the NBD1:ICL4 site. For the NBD1 domain, two sites were selected for the study because there is no consensus in the literature about the exact region where VX-445 might interact on this domain. The first site was selected using the DoGSiteScorer method (Volkamer et al., 2010, 2012), which is a grid-based pocket detection and druggability prediction method, available on Protein Plus Server (<https://proteins.plus>) (Fährrolfes et al., 2017; Schöning-Stierand et al., 2020). The second site was selected based on the region described by Baatallah and collaborators (Baatallah et al., 2021). In both cases, the three-dimensional structure of the NBD1 domain (PDB: 1XMJ) was used (Lewis et al., 2004) with a spherical constraint with a radius of 10 Å. After selecting the interaction sites, the systems were evaluated by applying the molecular docking algorithm MolDock (Thomsen and Christensen, 2006), based on a hybrid search algorithm, called guided differential evolution. For the NBD1:ICL4 site, the ligands VX-661 and LSO-39 were evaluated; and the VX-445, LSO-18, and LSO-24 were evaluated for the NBD1 domain sites (I and II). All dockings were performed with a population size of 200, max iterations of 2000, scaling factor of 0.5, crossover rate of 0.9, grid resolution of 0.3, and 20 runs.

2.10. Statistical analysis

All conditions were performed in at least three independent experiments. Data were analyzed using GraphPad Prism software (version 8.3, GraphPad, USA). Statistical comparisons between the conditions tested were assessed by the One-way ANOVA test followed by Dunnett's or Tukey's posthoc tests and the significance is represented by *P* values < 0.05.

3. Results

3.1. Identification of putative F508del-CFTR traffic correctors by a small-scale screening of triazole compounds and derivatives

In order to identify compounds capable of rescuing F508del-CFTR, we first performed a well-established HS-YFP microfluorimetric assay. This assay enables the determination of F508del-CFTR function by measuring the quenching rate of the HS-YFP as a result of Cl^-/I^- exchange across the membrane (refer to Experimental Procedures). For the primary screen, cells were treated with compounds (3 and 20 μM) for 24 h and then acutely stimulated for 30 min with Fsk + Gen. An increase in the HS-YFP quenching rate was detected for 8 out of 45 compounds (Fig. 1), of which four were effective at the two concentrations tested: LSO-18, LSO-24, LSO-28, and LSO-39 (Suppl. Fig. 1). To further assess the efficacy and potency of these four hits, cells were treated for 24 h at multiple concentrations in the range of 0.01–30 μM and the HS-YFP quenching rate was measured. The four compounds were demonstrated to be active in the low micromolar range (Table 1).

3.2. In silico ADME analysis

The pharmacokinetic properties of novel molecules are important features to be determined in the early phases of drug development to enable possible progression into the clinical trial. We assessed the *in silico* ADME properties of the four hits using the SwissADME software (Daina et al., 2017). The following physicochemical parameters were evaluated based on Lipinski's rule of five (Lipinski, 2004): molecular weight (MW), the calculated logarithm of the octanol-water partition coefficient (LogP), number of H-bond donors (nHBD), number of H-bond acceptors (nHBA) and number of rotatable bonds (nRB), along with the topological polar surface area (TPSA). In order to be considered an orally active drug candidate, Lipinski's rule of five states that a small molecule should have MW ≤ 500 Da, LogP ≤ 5, nHBD ≤ 5, nHBA ≤ 10, and nRB ≤ 10. Absorption and membrane permeability are also influenced by TPSA, which should be ≤ 140 Å² to have gastrointestinal absorption. Table 1 depicts *in vitro* pharmacokinetic properties of compounds LSO-18, LSO-24, LSO-28, and LSO-39. The four compounds follow the Lipinski's rule and have a TPSA ≤ 140 Å², thus suggesting they have good gastrointestinal absorption. Moreover, they were not identified by pan-assay interference structures (PAINS), i.e., frequent hitters or "promiscuous" molecules that contain substructures demonstrating potent response in assays regardless of the target.

3.3. Validation of F508del-CFTR rescue by the four hit compounds

Next, we performed complementary assays to validate the effects of

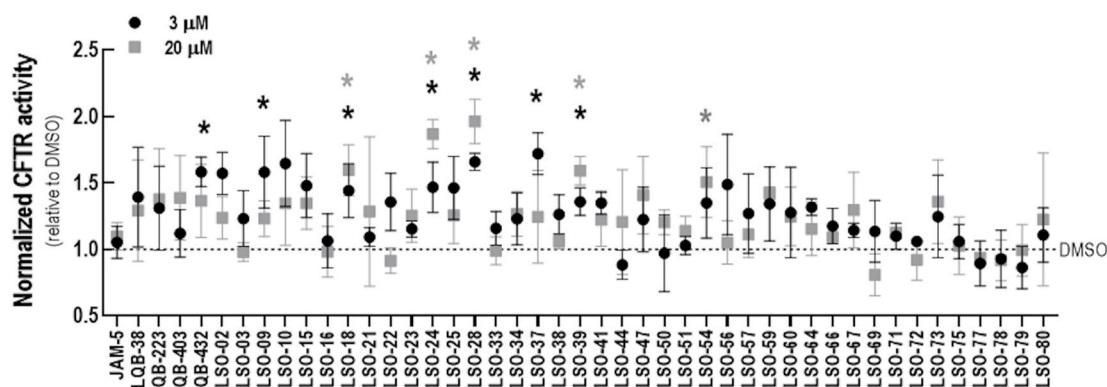


Fig. 1. Primary screen of triazole compounds. CFBE cells co-expressing F508del-CFTR and the HS-YFP were treated with compounds for 24h and then acutely stimulated (30 min) with Fsk (20 μM) and Gen (50 μM). CFTR function was assessed based on the rate of HS-YFP quenching and normalized to the negative control (DMSO, dashed line). Data are shown as means + SD of 4 independent experiments. vs. DMSO: **P* < 0.05.

Table 1Dose-response relationship^a and *in silico* analysis of absorption, distribution, metabolism and excretion (ADME).^b

Comp	EC ₅₀ (μM) ^a	MW ^b	LogP ^b	nHBD ^b	nHBA ^b	nRD ^b	TPSA (Å ²) ^b	GI absorption ^b	PAINS alert ^b
LSO-18	3.0	411.09	3.65	1	3	3	48.19	High	0
LSO-24	2.7	411.09	3.65	1	3	3	48.19	High	0
LSO-28	1.9	281.31	2.16	1	4	5	60.17	High	0
LSO-39	4.2	366.64	3.43	1	3	3	49.18	High	0

MW: molecular weight; LogP: values correspond to Consensus LogP_{w/o}; nHBD: number of H-bond donors; nHBA: number of H-bond acceptors; nRD: number of rotatable bonds; TPSA: topological polar surface area; GI: gastrointestinal; PAINS: pan-assay interference structures.

^a Data obtained by the HS-YFP quenching experiments.

^b Data obtained by using SwissADME software.

LSO-18, LSO-24, LSO-28, and LSO-39 in rescuing F508del-CFTR processing, PM trafficking, and function. The clinically approved correctors VX-661 and VX-445 were tested in parallel as positive controls for F508del-CFTR rescue. Incubation of CFBE cells expressing F508del-CFTR with 10 μM of each of the hit compounds rescued F508del-CFTR processing (Fig. 2A and B), as evidenced by the appearance of the fully-glycosylated form of CFTR (170–180 kDa, band C), in contrast to DMSO (negative control), which only led to the appearance of the core-glycosylated form of CFTR (140–150 kDa, band B). Rescue of F508del-CFTR processing by LSO-18, LSO-24, and LSO-39 was comparable to that obtained for VX-661 (2.1–2.6-fold increase vs. DMSO), while it was superior for LSO-28 and VX-445 (3.1–4.2-fold increase vs. DMSO).

To assess rescue of F508del-CFTR PM trafficking, immunofluorescence microscopy was performed to detect extracellularly exposed Flag-tag of mCherry-Flag-F508del-CFTR expressed in CFBE cells without cell permeabilization (Fig. 2C). After 24 h incubation with either LSO-18, LSO-24, LSO-28, LSO-39, VX-661, or VX-445, the appearance of an anti-Flag signal was detected (Fig. 2D), indicating that F508del-CFTR PM expression was rescued, albeit at different efficacy levels depending on the treatment. LSO-18, LSO-24, and LSO-39 showed an effect comparable to that of VX-661, while LSO-28 and VX-445 exhibited greater rescue. However, the mCherry fluorescence signal was similar to that in cells incubated with DMSO, indicating that none of these compounds induced changes in the total amount of CFTR (Fig. 2E).

The rescue of F508del-CFTR function was further confirmed by the HS-YFP quenching rate in CFBE cells co-expressing F508del-CFTR and the HS-YFP. Upon Fsk + Gen stimulation, there was a significant decay in fluorescence of cells incubated with LSO-18, LSO-24, LSO-28, LSO-39, VX-661, or VX-445, indicating HS-YFP quenching promoted by I⁻ influx through F508del-CFTR (Fig. 2F and G). Again, such effects were higher for LSO-28 and VX-445 (2.6–3.2-fold increase vs. DMSO) compared to LSO-18, LSO-24, LSO-39, and VX-661 (1.7–2.3-fold increase vs. DMSO).

3.4. Functional rescue of F508del-CFTR by triazole compounds in micro-Ussing chamber measurements

The ability of LSO-18, LSO-24, LSO-28, and LSO-39 to rescue F508del-CFTR function was further validated in polarized monolayers of CFBE cells in the Ussing chamber (Fig. 3). Compared to DMSO, an increase in equivalent short-circuit current ($\Delta I_{sc_{eq}}$) was evidenced upon Fsk + Gen stimulation in cells incubated for 24 h with VX-661, LSO-18, LSO-24 and LSO-28 (3.9, 2.7, 3.5 and 8.1-fold increase) (Fig. 3A–E). These increases were abolished by adding CFTRinh-172, indicating that they are CFTR-specific. LSO-39 showed no significant increase in $\Delta I_{sc_{eq}}$ compared to DMSO (Fig. 3A,F). However, a significantly higher $\Delta I_{sc_{eq}}$ (~17-fold increase) was observed for cells incubated with VX-661+VX-445 (Fig. 3G–I).

3.5. Additivity of hit compounds with the clinically approved correctors in rescuing F508del-CFTR

We then investigated whether additional F508del-CFTR rescue could be achieved by the combination of triazole compounds with the

clinically approved correctors VX-661 and VX-445. CFBE cells expressing F508del-CFTR were incubated for 24 h with compounds, individually or combined, and F508del-CFTR processing and function were assessed in CFBE cells without and with HS-YFP co-expression, respectively. LSO-18, LSO-24, and LSO-28, but not LSO-39, showed additive rescue of F508del-CFTR processing (4.1–7.9-fold increase vs. DMSO) (Fig. 4A and B) and function (3.4–4.3-fold increase vs. DMSO) in combination with VX-661 (Fig. 4D,F). On the other hand, LSO-28 and LSO-39, but not LSO-18 nor LSO-24, presented additivity in combination with VX-445, as observed by the increase in F508del-CFTR processing (~10-fold increase vs. DMSO) (Fig. 4A,C) and the HS-YFP quenching rate (~6-fold increase vs. DMSO) (Fig. 4E,G).

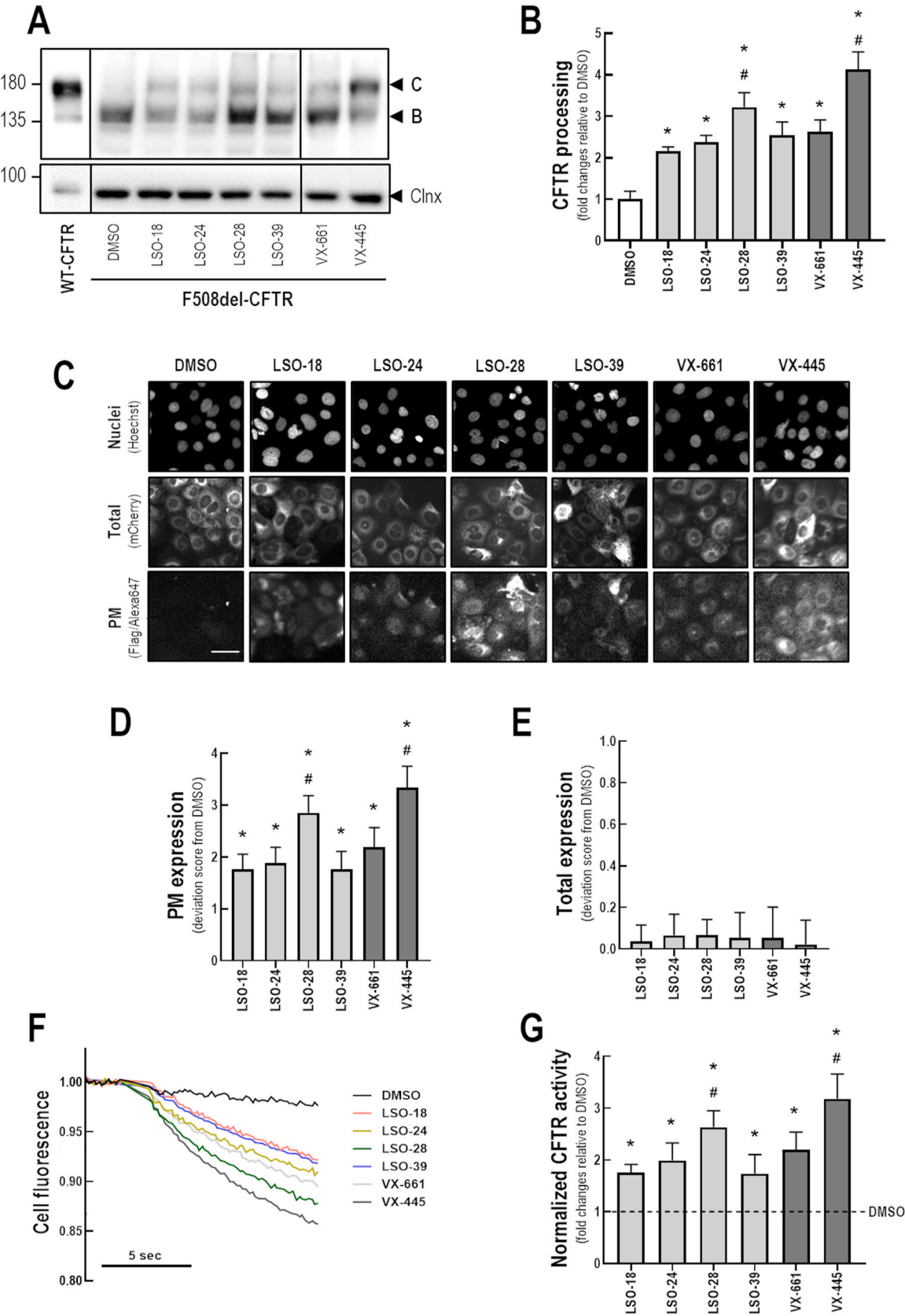
Next, we assessed the extent of F508del-CFTR rescue by a triple combination of VX-661 plus VX-445 with LSO-18, LSO-24, LSO-28, or LSO-39 (Suppl. Fig. 2). However, the data show that rescue of F508del-CFTR processing and function achieved by any of these triple combinations was comparable to levels of rescue by VX-661+VX-445 double combination.

3.6. Additive effects of triazole compounds and low temperature in rescuing F508del-CFTR

To shed some light on the MoA by which these compounds rescue F508del-CFTR processing and function, we tested their effects under low-temperature incubation (27 °C). CFBE cells expressing F508del-CFTR with and without the co-expression of the HS-YFP were cultured at 27 °C for 24 h and then kept for an additional 24 h-period at 27 °C in the presence of DMSO, LSO-18, LSO-24, LSO-28, LSO-39, VX-661, or VX-445. Cells incubated with DMSO at 27 °C showed rescue of F508del-CFTR processing compared to those at 37 °C, as expected. A further increase in F508del-CFTR processing was observed in cells kept at 27 °C and incubated with LSO-18, LSO-24, LSO-28, LSO-39, VX-661 or VX-445 (1.8–2.5-fold increase) compared to those incubated with DMSO also at 27 °C (Suppl. Fig. 3A and B). Rescue of F508del-CFTR processing by LSO-28 and VX-445 at 27 °C was greater (1.4-fold increase) in comparison to that by VX-661 at low temperature. A similar behavior was observed in the HS-YFP assay (Suppl. Fig. 3C and D). Under low-temperature incubation, F508del-CFTR function was increased in cells incubated with LSO-18, LSO-24, LSO-28, LSO-39, VX-661, or VX-445 (1.2–1.4-fold increase) compared to DMSO with a higher fluorescence decay evidenced by LSO-28 and VX-445.

3.7. MoA of F508del-CFTR rescue by triazole compounds by additivity with genetic revertants of F508del-CFTR and null-traffic DD/AA-CFTR variant

One way to gain further understanding of the MoA of these compounds in the rescue of F508del-CFTR is to look into their potential additive effects on the processing and function of well-characterized genetic revertants of this mutant. To this end, CFBE cells expressing F508del-CFTR *in cis* with the revertant G550E, R1070W, 4RK or expressing the null-traffic DD/AA-CFTR (either with or without co-expression of the HS-YFP) were incubated for 24 h with LSO-18, LSO-



(caption on next page)

Fig. 2. Validation of the effects of triazole compounds in the rescue F508del-CFTR by biochemical, immunofluorescence microscopy, and functional assays. (A) Representative WB images of CFBE cells expressing WT- or F508del-CFTR treated for 24 h with DMSO (negative control), LSO-18 (10 μ M), LSO-24 (10 μ M), LSO-28 (10 μ M), LSO-39 (10 μ M), VX-661 (5 μ M) or VX-445 (3 μ M). (B) CFTR processing [band C/bands B + C] was quantified and normalized to calnexin (Clnx) levels (loading control). Data are shown as means + SD of 4 independent experiments. vs. DMSO: * P < 0.05; vs. VX-661: # P < 0.05. (C) Representative fluorescence images of CFBE cells expressing mCherry-Flag-F508del-CFTR treated with compounds for 24 h. The extracellularly exposed Flag-tags and mCherry-tags were quantified to determine (D) CFTR located at the PM and (E) the total amount of CFTR in cells, respectively. Data are shown as deviation score + SD of 4 independent experiments. vs. DMSO: * P < 0.05; vs. VX-661: # P < 0.05. (F) Representative cell fluorescence recording on a plate reader. CFBE cells co-expressing F508del-CFTR and the HS-YFP were treated with compounds for 24 h and then acutely stimulated (30 min) with Fsk (20 μ M) and Gen (50 μ M). (G) CFTR function was assessed based on the rate of HS-YFP quenching and normalized to the negative control (DMSO, dashed line). Data are shown as means + SD of 4 independent experiments. vs. DMSO: * P < 0.05; vs. VX-661: # P < 0.05.

24, LSO-28, LSO-39, VX-661, or VX-445. F508del/G550E-CFTR processing (2–2.5-fold increase vs. DMSO) and function (1.5 to 2-fold increase vs. DMSO) were increased in cells incubated with any of these compounds (Fig. 5A–D). In cells expressing F508del/R1070W-CFTR, LSO-18, LSO-24, LSO-28, and VX-445, but not LSO-39 and VX-661, increased its processing (2–2.6-fold increase vs. DMSO) and function (1.6 to 2-fold increase vs. DMSO) (Fig. 5E–H). Incubation of cells with any of these compounds increased F508del/4RK-CFTR processing (2.1–3.9-fold increase vs. DMSO) and function (1.7–3.2-fold increase vs. DMSO), with a further increase in processing observed for LSO-18, LSO-24, and VX-445, while these three compounds in addition to LSO-28 also showed higher F508del/4RK-CFTR function compared to that for VX-661 (Fig. 6A–D). On the other hand, none of the compounds tested was able to rescue DD/AA-CFTR processing or function (Fig. 6E–H).

3.8. Molecular docking studies

The interactions of LSO-39, and VX-661 (as reference) with the NBD1:ICL4 binding site, and LSO-18, LSO-24, and VX-445 (as reference) with the NBD1 (I and II) binding sites were investigated with molecular docking to obtain the MolDock score, the hydrogen bond energy contribution, and the interaction energy of the protein-ligand complex, as presented in Table 2. In the NBD1:ICL4 binding site, VX-661 was demonstrated to interact with residues Trp496, Met498, Lys503, Asn505, Ile507, and Val510, while LSO-39 interacts with Tyr1073 (Suppl. Fig. 4A and B). Based on the site with the highest conformation prevalence according to the protein plus server (i.e., NBD1 site I), VX-445 might interact with the residues Gln493 and Tyr557 along with a molecule of water (Suppl. Fig. 4C). In our docking studies, only the residue Gln637 demonstrated a hydrogen bond with VX-445 (Suppl. Fig. 4D) of all residues presented in a previous publication (Baatallah et al., 2021). LSO-18 and LSO-24 also show hydrogen bond with Gln637, indicating that this residue may be important for the stability of the ligands at this site (Suppl. Fig. 4E and F). We also found that VX-445 presents hydrogen bonds with the residue Arg668, while LSO-24 interacts with the residue Phe640.

3.9. Rescue of rare CFTR mutations by triazole compounds

To interrogate the potential utility of LSO-18, LSO-24, LSO-28, and LSO-39 in rescuing rare CF-causing mutations, CFBE cells expressing G85E-, L206W-, R334W-, I507del-, R560S- or N1303K-CFTR were treated for 24 h with these compounds and WB analysis was performed (Fig. 7). In L206W-expressing cells, treatment with any of these compounds led to the appearance of the fully-glycosylated form of CFTR, with LSO-18 and LSO-39 more effective than LSO-24 and LSO-28 (Fig. 7B,G). These compounds were also effective at increasing CFTR processing in R334W-expressing cells (Fig. 7C,G). However, there was no rescue of the processing of G85E-, I507del-, R560S- and N1303K-CFTR by triazole compounds, similarly to DMSO, thus only the core-glycosylated immature form of CFTR was detected (Fig. 7A,D,F).

4. Discussion

Identification of novel drugs capable of correcting F508del-CFTR

trafficking defect is crucial to develop causative therapies for the majority of individuals with CF (80–85% worldwide). Nevertheless, it is generally accepted that a single compound may be insufficient to rescue F508del-CFTR protein at therapeutically relevant levels, since this mutation promotes multiple structural defects on the CFTR protein (Dalemans et al., 1991; Jensen et al., 1995; Lopes-Pacheco, 2020; Sharma et al., 2001). In this context, the double corrector combination VX-445/VX-661 demonstrated superior rescue of F508del-CFTR processing and trafficking compared to each corrector individually (Capurro et al., 2021; Veit et al., 2020). Furthermore, these drugs (in combination with the potentiator VX-770) have recently been granted by the FDA a label extension to additional 177 CF-causing mutations based on *in vitro* data in FRT cell lines (Costa et al., 2022; Lopes-Pacheco et al., 2021). Despite such impressive progress, this triple combo drug only partially rescues F508del-CFTR (Capurro et al., 2021), indicating that there is still scope for further improvements. Moreover, some CFTR mutations with similar functional defects as F508del are not at all or only modestly rescued (i.e., sub-clinically relevant levels) by existing modulators (Dekkers et al., 2016; Lopes-Pacheco et al., 2016, 2017; Pedemonte et al., 2005; Ramalho et al., 2022; Rapino et al., 2015; Veit et al., 2020). Accordingly, the identification of novel correctors is yet required not only to achieve more robust clinical benefits, likely as drug combinations, but also to minimize the financial burden with alternative therapeutic options.

To look into the utility of novel triazole compounds as potential drug candidates for CF, we carried out a series of experiments to determine their efficacy in the rescue of F508del-CFTR. Initially, CFBE cells expressing F508del-CFTR together with the HS-YFP were treated with compounds for 24 h to assess F508del-CFTR functional rescue, as previously extensively described to identify novel CFTR modulators (Capurro et al., 2021; Lopes-Pacheco et al., 2020, 2022; Pedemonte et al., 2005; Sondo et al., 2011; Veit et al., 2018). Four hits were identified in the primary screen (LSO-18, LSO-24, LSO-28, and LSO-39) by demonstrating to be putatively active at the two concentrations tested. Subsequent biochemical, immunofluorescence, and functional data confirmed the ability of these compounds to rescue F508del-CFTR, as respectively indicated by the appearance of the mature, fully-glycosylated (post-Golgi) CFTR form, detection of anti-Flag signal at the PM, and CFTR-dependent Cl[−] currents in micro-Ussing chamber measurements. Because no changes were found in total F508del-CFTR expression, it is unlikely that the rescue by these compounds resulted from increased CFTR translation efficiency. Regarding potency, these triazole compounds have a higher EC₅₀ (1.9–4.2 μ M) compared to other correctors already in the clinic for CF, namely VX-809 and VX-661 (EC₅₀: ~250 and ~580 nM, respectively) (Singh et al., 2020), despite their equivalent rescuing efficacies. Moreover, these investigational compounds do not violate Lipinski's rule of five for drug-like molecules (Lipinski, 2004) and are therefore expected to have good bioavailability.

The F508del-CFTR protein is temperature sensitive (Sharma et al., 2001; Wang et al., 2008) and incubation of cells expressing this mutant at a lower temperature (26–30 °C) than the human physiological one (37 °C) yields a “permissive” proteostasis environment and an energetically favorable F508del-CFTR folding (Denning et al., 1992; Lopes-Pacheco et al., 2015). This leads to accumulation of its immature form in the ER and subsequent trafficking to the PM, likely by saturating the

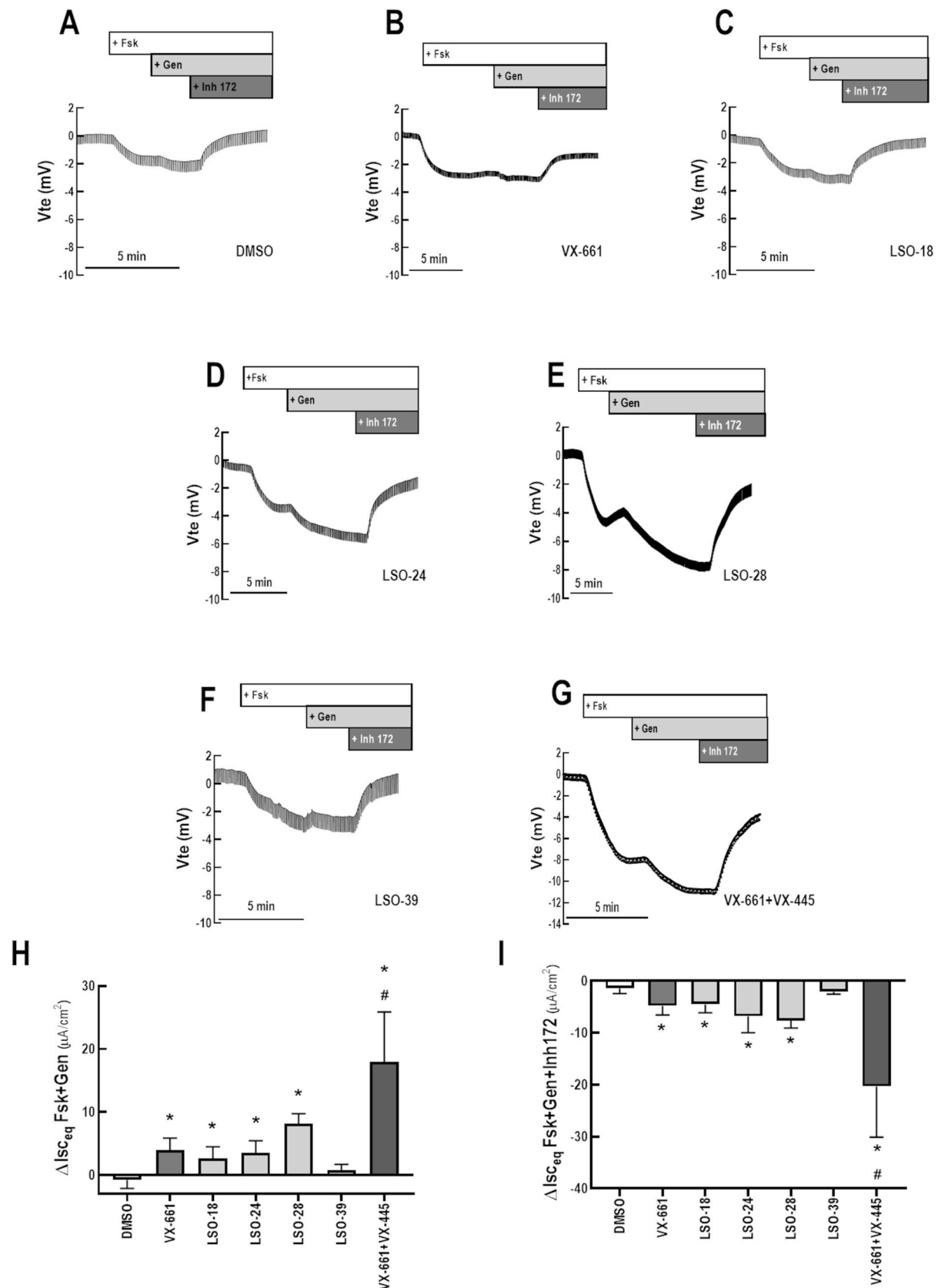


Fig. 3. Rescue of F508del-CFTR function by triazole compounds in micro-Ussing chamber measurements. Representative Ussing chamber (open-circuit) recordings depicting transepithelial voltage measurements (V_{te}) of polarized monolayers of CFBE cells expressing F508del-CFTR treated for 24h with (A) DMSO (negative control), (B) VX-661 (5 μ M), (C) LSO-18 (10 μ M), (D) LSO-24 (10 μ M), (E) LSO-28 (10 μ M), (F) LSO-39 (10 μ M), and (G) VX-661+VX-445 (5 μ M and 3 μ M, respectively). Data are represented as (F) mean increase in I_{eq-sc} induced by Fsk (2 μ M) plus Gen (50 μ M), and (I) mean inhibition in I_{eq-sc} by CFTRinh-172 (30 μ M). Data are shown as means + SD of 3–5 independent experiments for each condition. vs. DMSO: * P < 0.05; vs. VX-661: # P < 0.05.

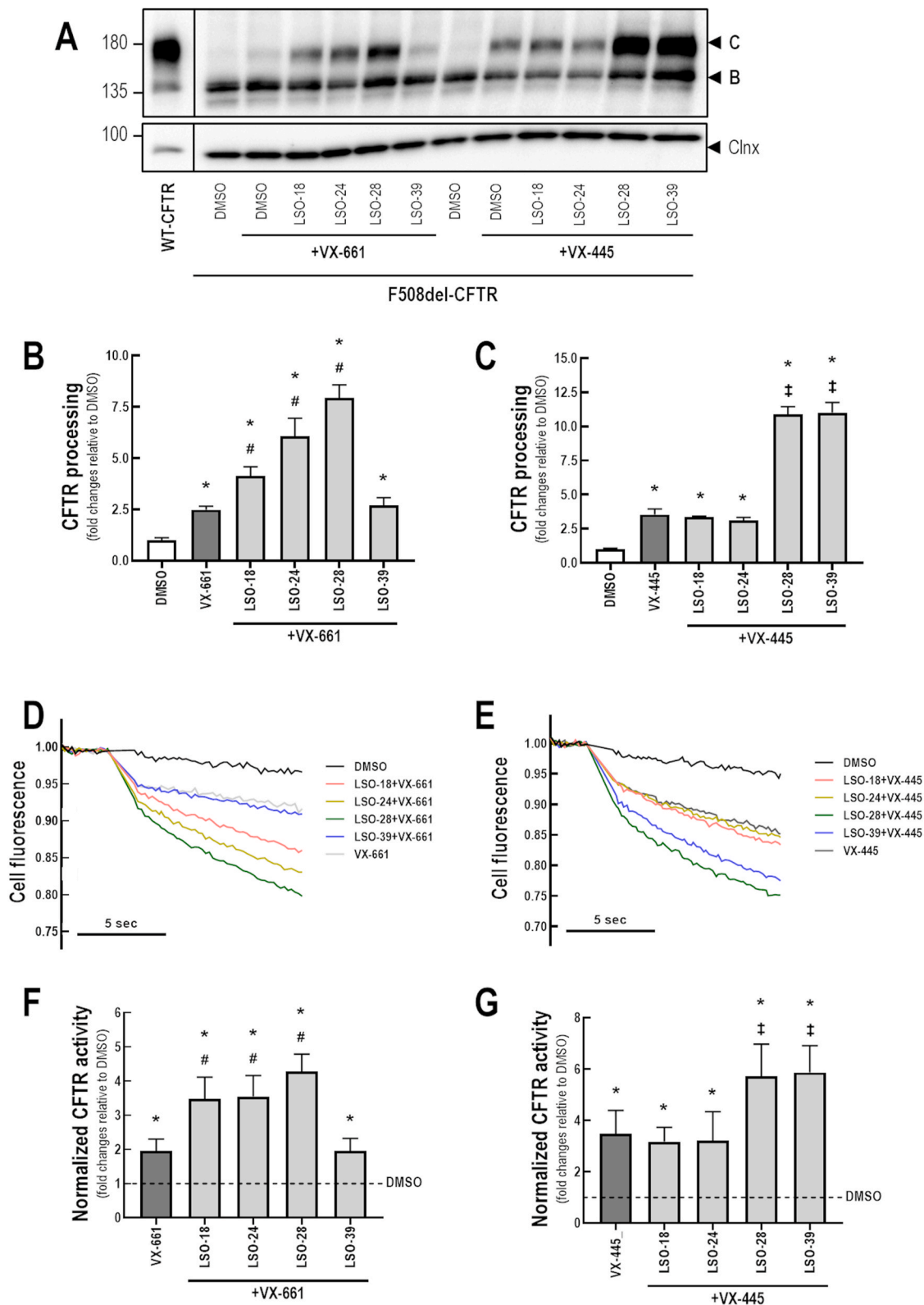


Fig. 4. Assessment of the additive effects of triazole compounds with VX-661 or VX-445 in the rescue of F508del-CFTR. (A) Representative WB images of CFBE cells expressing WT- or F508del-CFTR treated for 24 h with DMSO (negative control), VX-661 (5 μ M), or VX-445 (3 μ M) individually or in combination with LSO-18 (10 μ M), LSO-24 (10 μ M), LSO-28 (10 μ M) and LSO-39 (10 μ M). (B,C) CFTR processing [band C/bands B + C] was quantified and normalized to calnexin (Clnx) levels (loading control). Data are shown as means \pm SD of 4 independent experiments. vs. DMSO: * P < 0.05; vs. VX-661: # P < 0.05; vs. VX-445: ‡ P < 0.05. (D,E) Representative cell fluorescence recording on a plate reader. CFBE cells co-expressing F508del-CFTR and the HS-YFP were treated with compounds for 24h and then acutely stimulated (30 min) with Fsk (20 μ M) and Gen (50 μ M). (F,G) CFTR function was assessed based on the rate of HS-YFP quenching and normalized to the negative control (DMSO, dashed line). Data are shown as means \pm SD of 4 independent experiments. vs. DMSO: * P < 0.05; vs. VX-661: # P < 0.05; vs. VX-445: ‡ P < 0.05.

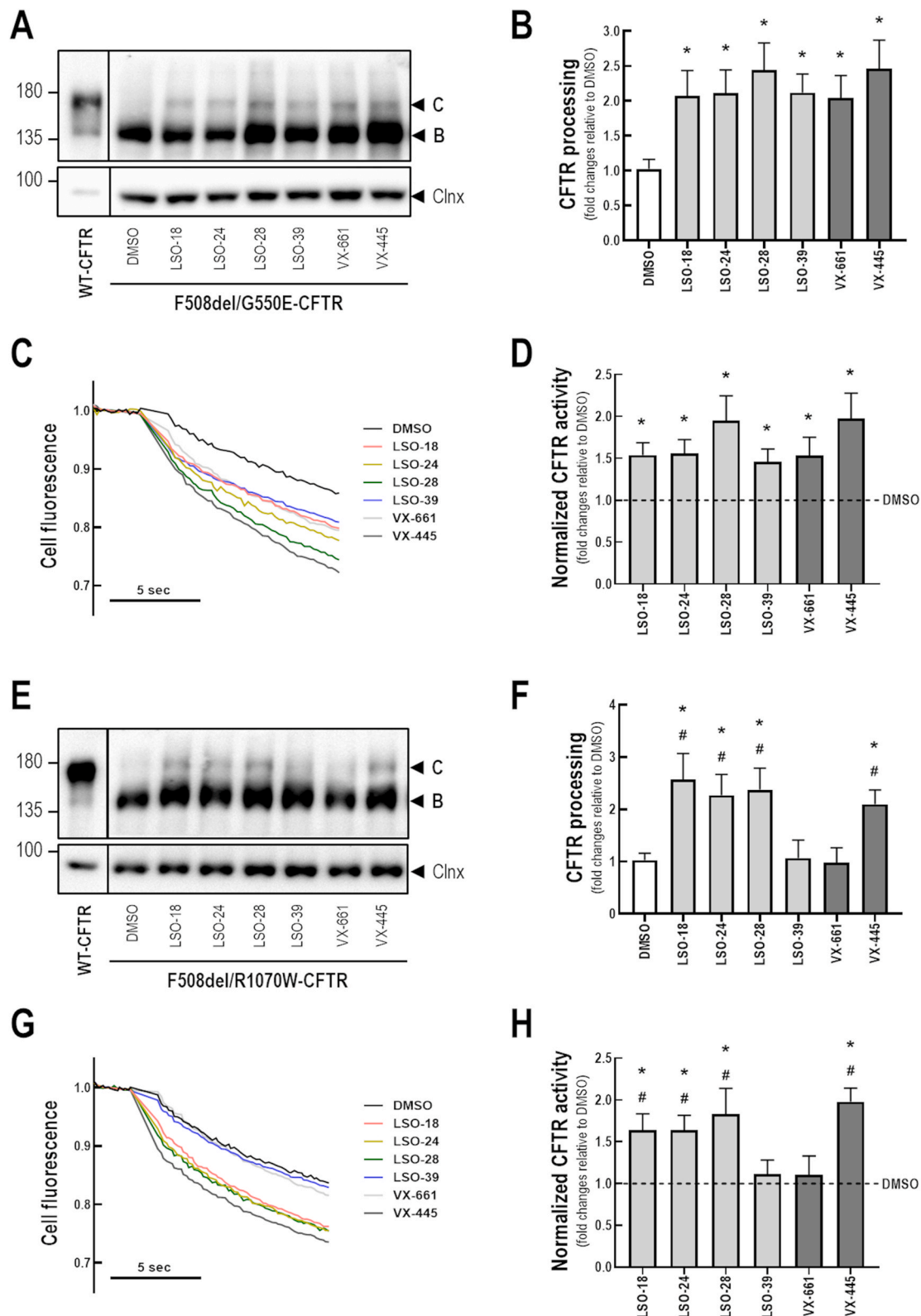


Fig. 5. Effect of triazole compounds in the F508del-CFTR genetic revertants G550E and R1070W. Representative WB images of CFBE cells expressing WT-, (A) F508del/G550E- or (E) F508del/R1070W-CFTR treated for 24h with DMSO (negative control), LSO-18 (10 μ M), LSO-24 (10 μ M), LSO-28 (10 μ M), LSO-39 (10 μ M), VX-661 (5 μ M) or VX-445 (3 μ M). (B,F) CFTR processing [band C/bands B + C] was quantified and normalized to calnexin (Clnx) levels (loading control). Data are shown as means + SD of 4 independent experiments. vs. DMSO: * P < 0.05; vs. VX-661: # P < 0.05. Representative cell fluorescence recording on a plate reader. CFBE cells co-expressing the HS-YFP and (C) F508del/G550E-CFTR or (G) F508del/R1070W-CFTR were treated with compounds for 24 h and then acutely stimulated (30 min) with Fsk (20 μ M) and Gen (50 μ M). (D,H) CFTR function was assessed based on the rate of HS-YFP quenching and normalized to the negative control (DMSO, dashed line). Data are shown as means + SD of 4 independent experiments. vs. DMSO: * P < 0.05; vs. VX-661: # P < 0.05.

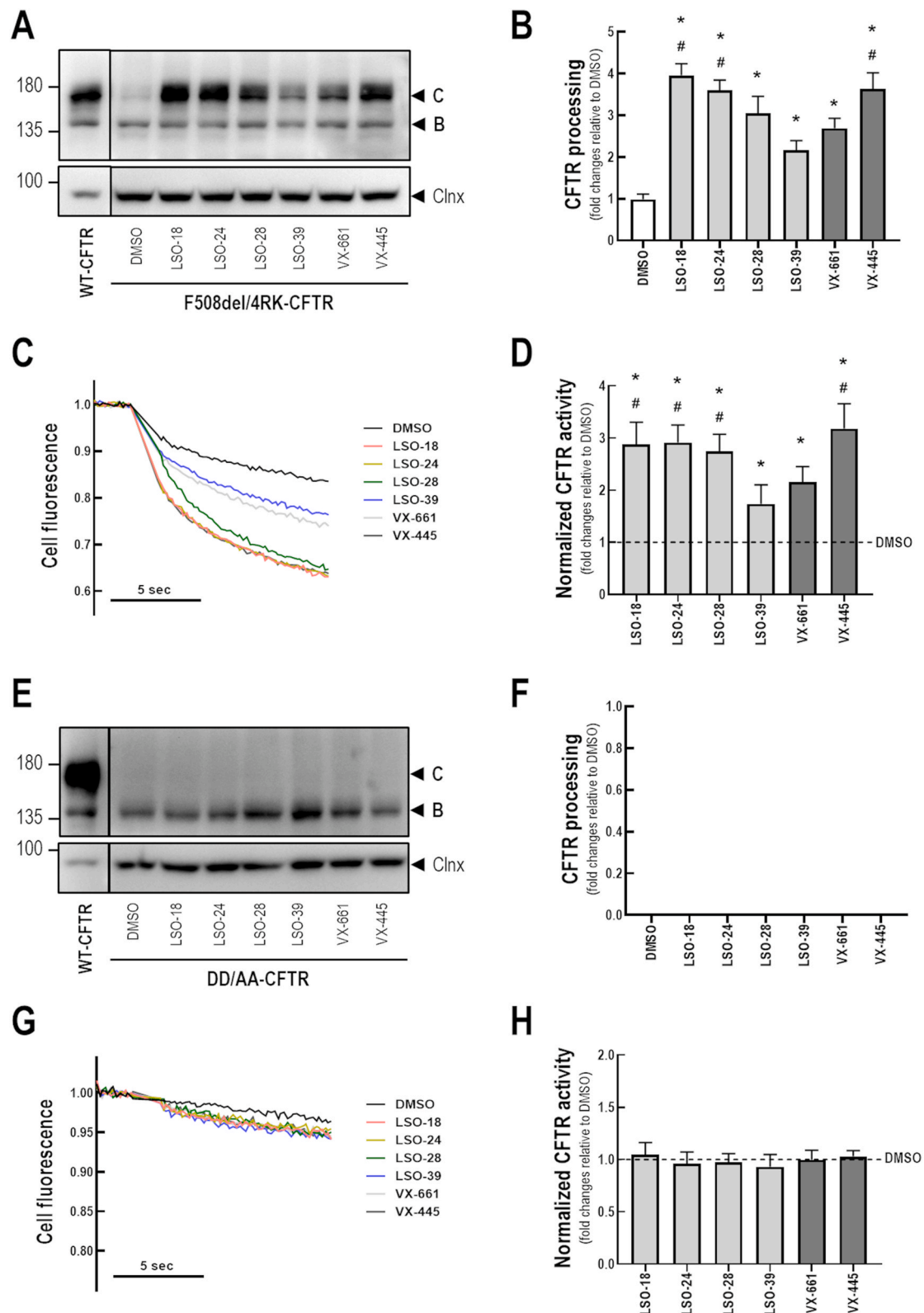


Fig. 6. Effect of triazole compounds in the F508del-CFTR genetic revertant 4RK and the null-traffic DD/AA variant. Representative WB images of CFBE cells expressing WT-, (A) F508del/4RK- or (E) DD/AA-CFTR treated for 24 h with DMSO (negative control), LSO-18 (10 μ M), LSO-24 (10 μ M), LSO-28 (10 μ M), LSO-39 (10 μ M), VX-661 (5 μ M) or VX-445 (3 μ M). (B,F) CFTR processing [band C/bands B + C] was quantified and normalized to calnexin (Clx) levels (loading control). Data are shown as means + SD of 4 independent experiments. vs. DMSO: * P < 0.05; vs. VX-661: # P < 0.05. Representative cell fluorescence recording on a plate reader. CFBE cells co-expressing the HS-YFP and (C) F508del/4RK-CFTR or (G) DD/AA-CFTR were treated with compounds for 24 h and then acutely stimulated (30 min) with Fsk (20 μ M) and Gen (50 μ M). (D,H) CFTR function was assessed based on the rate of HS-YFP quenching and normalized to the negative control (DMSO, dashed line). Data are shown as means + SD of 4 independent experiments. vs. DMSO: * P < 0.05; vs. VX-661: # P < 0.05.

Table 2
Parameters determined by molecular docking studies.

Site	Ligand	Moldock Score (Kcal.mol ⁻¹)	H-bond (Kcal.mol ⁻¹)	Interaction (Kcal.mol ⁻¹)
NBD1: ICL4	VX-661	-120.31	-14.92	-120.81
	LSO-39	-93.53	-2.36	-94.79
NBD1 (I)	VX-445	-126.88	-3.80	-112.04
NBD1 (II)	VX-445	-127.62	-6.55	-121.00
	LSO-18	-94.18	-5.20	-97.06
	LSO-24	-94.44	-7.10	-107.80

Molecular docking results were obtained by applying the Moldock algorithm with the values of the scoring function (Moldock Score), the energy values assigned to hydrogen bonds (H-bond) and the energy values assigned exclusively from the protein and ligand interaction for the NBD1:ICL4, NBD1 (I), and NBD1 (II) sites.

ERQC (Farinha et al., 2013). Our biochemical and functional data demonstrated that LSO-18, LSO-24, LSO-28, and LSO-39 as well as VX-661 and VX-445 are additive to low temperature in rescuing F508del-CFTR, pointing thus to distinct mechanisms employed by these chemical agents. Similar effects were previously reported for several correctors, including C18, VX-809 (both similar drugs to VX-661), VRT-325, Corr-4a, and RDR01752 (Farinha et al., 2013; Lopes-Pacheco et al., 2015, 2020; Sondo et al., 2011). However, no additivity to low temperature was observed for ouabain or MCG1516A, which were suggested to operate via a similar mechanism to that of low temperature in rescuing F508del-CFTR (Lopes-Pacheco et al., 2022; Zhang et al., 2012).

Although the MoA of clinically approved CFTR modulators is not entirely elucidated, significant advances have been made to understand how these drugs correct F508del-CFTR defects (Baatallah et al., 2021; Capurro et al., 2021; Farinha et al., 2013; Fiedorczuk and Chen, 2022; Veit et al., 2020). We examined the additivity of the four hit compounds to VX-661 and VX-445 to interrogate whether they act by similar or complementary mechanisms. Our data indicate that LSO-39 shares a common mechanism with VX-661, while LSO-18, LSO-24, and VX-445

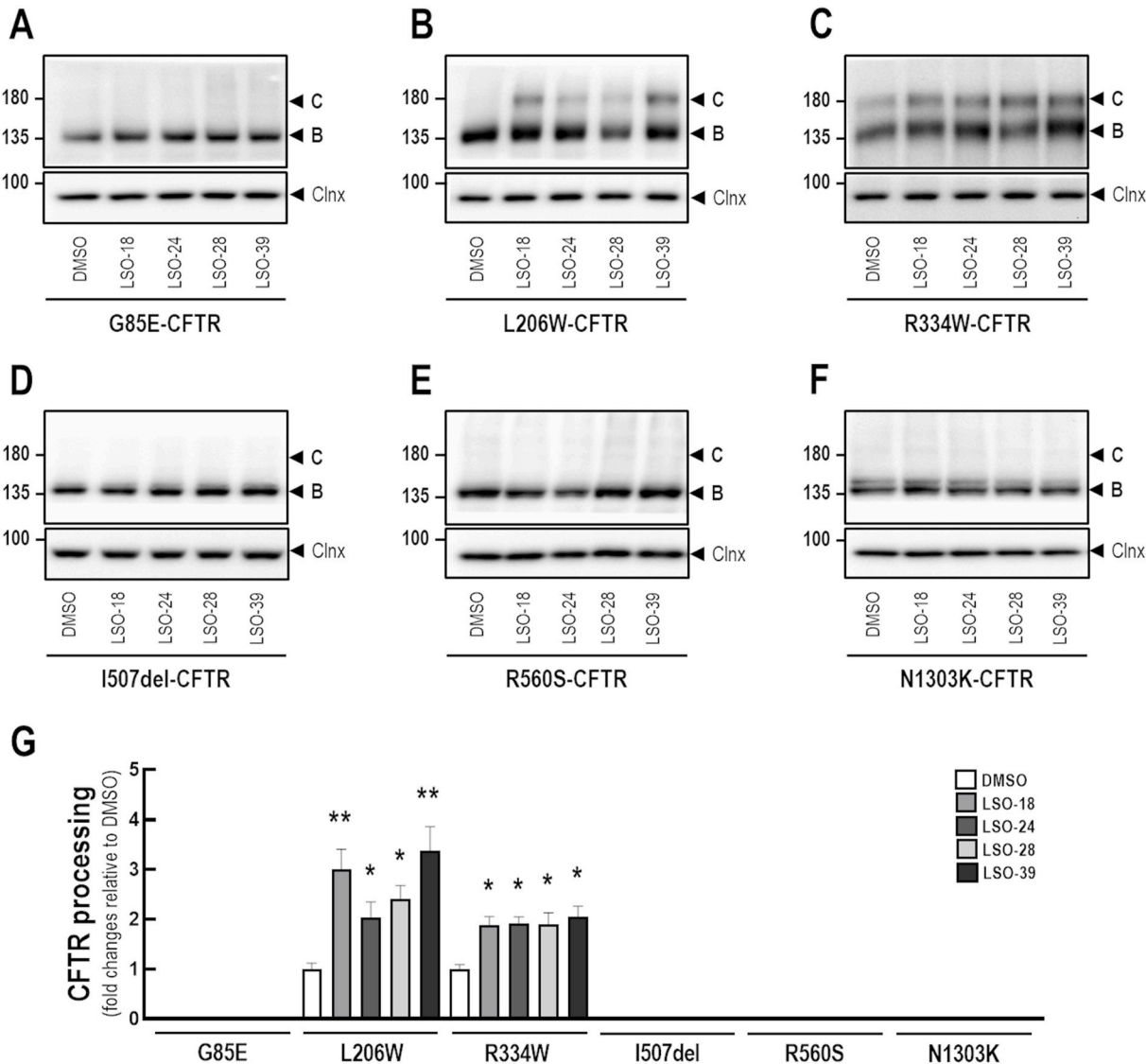


Fig. 7. Rescue of rare CFTR mutations by triazole compounds. Representative WB images of CFBE cells expressing (A) G85E-, (B) L206W-, (C) R334W-, (D) I507del-, (E) R560S- or (F) N1303K-CFTR treated for 24h with DMSO (negative control), LSO-18 (10 μ M), LSO-24 (10 μ M), LSO-28 (10 μ M) or LSO-39 (10 μ M). (G) CFTR processing [band C/bands B + C] was quantified and normalized to calnexin (Clx) levels (loading control). Data are shown as means + SD of 3 independent experiments. vs. DMSO: * P < 0.05.

act in a similar way. Such findings are further supported by molecular docking assessments. Based on the lack of additivity of compound combinations, previous studies have also reported that C18, VX-809, ABBV-2222, and RDR01752 exhibit a common MoA with VX-661 (Baatallah et al., 2021; Fiedorczuk and Chen, 2022; Lopes-Pacheco et al., 2020; Singh et al., 2020; Veit et al., 2020), and compound 4172 with VX-445 (Capurro et al., 2021; Veit et al., 2020) in rescuing F508del-CFTR. Here, we found that LSO-28 is additive to either VX-661 or VX-445 in double corrector combinations; however, no further correction of F508del-CFTR was observed when these compounds were used in a triple combination in comparison to VX-445 plus VX-661. The inability of LSO-28 to bypass this efficacy ceiling may be explained by the potential allosteric effects of VX-445 plus VX-661 on the global F508del-CFTR conformation defect (Baatallah et al., 2021; Veit et al., 2020), which may correct the same F508del-CFTR defect as LSO-28.

To shed further light on the MoA of LSO-18, LSO-24, LSO-28, and LSO-39, we examined their additivity to genetic revertants (G550E, R1070W, and 4RK), which partially rescue F508del-CFTR by different mechanisms. The revertants G550E and R1070W are proposed to restore two distinct interdomain contact points in the three-dimensional structure of CFTR that are abolished by the absence of F508 residue at the NBD1 surface (Decarvalho et al., 2002; Prins et al., 2022; Rabeh et al., 2012; Roxo-Rosa et al., 2006; Thibodeau et al., 2010). While G550E retrieves NBD1:NBD2 dimer interaction (also critical for channel gating by forming a salt bridge between the ATP binding site in NBD1 with other residues from NBD2) (Decarvalho et al., 2002; Roxo-Rosa et al., 2006), R1070W recovers NBD1:ICL4 interface by occupying the region vacated by the F508del, which has a major contribution to the molecular contact between NBD1:TMD2 (Prins et al., 2022; Rabeh et al., 2012; Thibodeau et al., 2010). Our data suggest a putative binding site for both LSO-39 and VX-661 at the NBD1:ICL4 interface, as these compounds were not additive to R1070W in rescuing F508del-CFTR processing and function. These data are also corroborated by the lack of additivity in rescuing F508del-CFTR by LSO-39 and VX-661 when co-administered. Similar findings were previously reported for VX-809, C18, and RDR01752 (Farinha et al., 2013; Hudson et al., 2017; Lopes-Pacheco et al., 2020). On the other hand, VX-661 (or its analog VX-809) was also reported to bind and stabilize TMD1 by other studies (Loo and Clarke, 2017; Ren et al., 2013), including cryo-EM using WT-CFTR structures (Fiedorczuk and Chen, 2022). As previously suggested (Baatallah et al., 2021; Veit et al., 2020), these compounds may have multiple binding sites and/or promote allosteric effects since they are able to rescue mutations distributed throughout CFTR protein. Furthermore, the ability of LSO-18, LSO-24, LSO-28, and LSO-39, as well as VX-661 and VX-445, to additively rescue F508del-CFTR with G550E indicate that these compounds may be mechanistically distant to VRT-325 and MCG1516A, as the latter two have been previously reported to act at the NBD1:NBD2 interface (Farinha et al., 2013; Lopes-Pacheco et al., 2022).

Besides G550E and R1070W, we assessed the effects of LSO-18, LSO-24, LSO-28, and LSO-39 on the 4RK revertant. When CFTR attains a native conformation, its four AFT motifs are hidden inside the protein, allowing it to be exported from the ER (Chang et al., 1999; Roxo-Rosa et al., 2006). However, in F508del-CFTR, these AFTs are exposed due to misfolding, leading to its ER retention and premature degradation. In the 4RK revertant, these four AFT retention motifs are disrupted by replacing an arginine to a lysine in each one, thus enabling some F508del-CFTR molecules to evade the ER (Chang et al., 1999; Roxo-Rosa et al., 2006). Our biochemical and functional data demonstrated an increase in CFTR processing and activity in F508del/4RK-expressing cells by the four triazole compounds as well as by VX-661 and VX-445, indicating that none of these compounds acts on AFT-dependent ER retention to rescue F508del-CFTR. The ER export of CFTR also relies on the presence of a diacidic code promoting Sec24-COPII interaction, which is abolished in the DD/AA-CFTR variant without affecting protein folding (Farinha et al., 2013; Roy et al., 2010; Wang et al., 2004). The compounds under investigation were unable to

surmount the DD/AA-CFTR, in contrast to low temperature that was previously reported to enable DD/AA-CFTR exit from the ER via conventional ER-to-Golgi traffic (Farinha et al., 2013; Lopes-Pacheco et al., 2020). A GRASP-mediated mechanism was proposed to rescue F508del-CFTR PM trafficking by bypassing the ER-to-Golgi pathway (Gee et al., 2011; Kim et al., 2016). However, since our investigational compounds were unable to rescue either DD/AA-CFTR processing or function, this implies that they do not act by promoting this Golgi-independent unconventional pathway. Altogether, our data suggest that the combination of triazole compounds with molecules that can overcome AFT-dependent retention signals and DD/AA defects would maximize the rescue of F508del-CFTR.

Since CF-causing mutations do not respond equally to the same CFTR corrector, even those with a similar trafficking defect as F508del-CFTR, i.e., class II (Lopes-Pacheco, 2020; Pinto et al., 2021; Silva et al., 2022; Veit et al., 2020), we investigated whether LSO-18, LSO-24, LSO-28, and LSO-39 could rescue other CFTR mutants. In CFBE cells expressing L206W-CFTR, treatment with these compounds rescued the complex-glycosylated form expression at variable efficacy. Although LSO-18 and LSO-24 are thought to act by the same mechanism in rescuing F508del-CFTR, they demonstrated different levels of correction for L206W-CFTR. This mutation was also demonstrated to be rescued by other experimental correctors (Lopes-Pacheco et al., 2022; Ren et al., 2013; Veit et al., 2018, 2021) with similar behavior for ABBV-2222 having greater correction efficacy in comparison to VX-809, VX-661, and FLD-169 (Veit et al., 2021). Furthermore, the triazole hit compounds were effective at increasing CFTR processing in R334W-expressing cells, which is a mutant with minimal trafficking impairment but decreased channel conductance that still enables residual function (Sheppard et al., 1993; Van Goor et al., 2014). Therefore, increasing its trafficking to the PM might be beneficial as it would result in further CFTR-dependent anion transport. However, CFTR processing was not rescued by LSO-18, LSO-24, LSO-28, or LSO-39 in G85E-, I507del-, R560S- and N1303K-expressing cells. These trafficking mutants were also refractory to several correctors in previous studies (Dekkers et al., 2016; Lopes-Pacheco et al., 2016, 2017; Pedemonte et al., 2005; Ramalho et al., 2022; Silva et al., 2021; Veit et al., 2018), although G85E and N1303K were recently demonstrated to be rescued by VX-445/VX-661/VX-770 at a lower level of that for F508del-CFTR (Veit et al., 2020). Altogether, these data suggest that triazole compounds may rescue L206W- and R334W-CFTR in addition to F508del-CFTR, but further investigation should be performed in patient-derived samples in future studies.

5. Conclusion

In summary, we identified four novel small molecules having a triazole scaffold that rescue F508del-CFTR traffic. Although drug development is a long process, requiring subsequent advancements in medicinal chemistry to reach compounds with greater potency and selectivity for clinical use, these hits provide a good starting point for further optimization. These four-hit compounds demonstrated similar efficacy to VX-661, although this compound alone promotes suboptimal effects. Regarding their MoA, our studies with compound combinations, low temperature, and genetic revertants of F508del-CFTR aided in clustering together compounds with similar/complementary pharmacological behavior. Indeed, the data suggest that LSO-39 and VX-661 have a putative binding site at the NBD1:ICL4 interface, while LSO-18, LSO-24, and VX-445 likely share a common mechanism. LSO-28, in contrast, appears to act by a different mechanism in comparison to the former compounds, although it does not further enhance the global F508del-CFTR conformation correction provided by VX-445 plus VX-661. Because none of these compounds rescue DD/AA traffic nor act on AFT-dependent retention signals, the combination of molecules targeting these mechanisms with our investigational compounds may be further exploited to maximize F508del-CFTR correction.

Credit author statement

M.B., Data curation, Formal analysis, Writing – original draft, Writing – editing. **F.C.F.**, Data curation, Formal analysis, Writing – editing. **A.K.**, Data curation. **F.R.S.**, Data curation, Formal analysis, Writing – editing. **V.D.S.**, Data curation. **A.S.P.**, Formal analysis, Writing – editing. **M.D.A.**, Conceptualization, Formal analysis, Writing – original draft, Writing – editing. **C.D.B.**, Conceptualization, Formal analysis, Writing – editing. **M.L.-P.**, Conceptualization, Formal analysis, Funding acquisition, Writing – original draft, Writing – editing. All authors read and approved the final version of the manuscript.

Funding

This work was supported by UIDB/04046/2020 and UIDP/04047/2020 center grants from FCT Portugal (to BioISI) and research grants: “2018 Research Scholars” from Gilead Sciences USA and “LOPES2110” from Cystic Fibrosis Foundation USA (both to M.L.-P.).

Declaration of competing interest

M.D.A., C.D.B. and M.L.-P. are inventors on a patent/patent application related to this work deposited at the Portuguese National Institute of Industrial Property (INPI). The other authors declare no conflict of interest.

Data availability

No data was used for the research described in the article.

Acknowledgments

The authors thank Sofia Correia (from BioISI) for technical support, Dr. Nicoletta Pedemonte (from IRCCS Istituto Giannina Gaslini, Italy) for kindly providing the HS-YFP pcDNA3.1 plasmid, and Cystic Fibrosis Foundation Therapeutics (CFFT, USA) for 596 anti-CFTR antibody.

Appendix A. Supplementary data

Supplementary data to this article can be found online at <https://doi.org/10.1016/j.ejphar.2022.175396>.

References

- Baatallah, N., Elbahnsi, A., Mornon, J.-P., Chevalier, B., Pranke, I., Servel, N., Zelli, R., Décourt, J.-L., Edelman, A., Sermet-Gaudelus, I., Callebaut, I., Hinzpeter, A., 2021. Pharmacological chaperones improve intra-domain stability and inter-domain assembly via distinct binding sites to rescue misfolded CFTR. *Cell. Mol. Life Sci.* 78, 7813–7829. <https://doi.org/10.1007/s00018-021-03994-5>.
- Bebok, Z., Collawn, J.F., Wakefield, J., Parker, W., Li, Y., Varga, K., Sorscher, E.J., Clancy, J.P., 2005. Failure of cAMP agonists to activate rescued $\Delta F508$ CFTR in CFBE41o- airway epithelial monolayers. *J. Physiol.* 569, 601–615. <https://doi.org/10.1113/jphysiol.2005.096669>.
- Berman, H.M., Westbrook, J., Feng, Z., Gilliland, G., Bhat, T.N., Weissig, H., Shindyalov, I.N., Bourne, P.E., 2000. The protein data bank. *Nucleic Acids Res.* 28, 235–242. <https://doi.org/10.1093/nar/28.1.235>.
- Bonandi, E., Christodoulou, M.S., Fumagalli, G., Perdicchia, D., Rastelli, G., Passarella, D., 2017. The 1,2,3-triazole ring as a bioisostere in medicinal chemistry. *Drug Discov. Today* 22, 1572–1581. <https://doi.org/10.1016/j.drudis.2017.05.014>.
- Botelho, H.M., Uliyakina, I., Awatade, N.T., Proença, M.C., Tischer, C., Sirianant, L., Kunzelmann, K., Pepperkok, R., Amaral, M.D., 2015. Protein traffic disorders : an effective high-throughput fluorescence microscopy pipeline for drug discovery. *Sci. Rep.* 12, 9038. <https://doi.org/10.1038/srep09038>.
- Capurro, V., Tomati, V., Sondo, E., Renda, M., Borrelli, A., Pastorino, C., Guidone, D., Venturini, A., Giraudo, A., Bertozzi, S.M., Musante, I., Bertozzi, F., Bandiera, T., Zara, F., Galletta, L.J.V., Pedemonte, N., 2021. Partial rescue of $\Delta F508$ -cftr stability and trafficking defects by double corrector treatment. *Int. J. Mol. Sci.* 22, 5262. <https://doi.org/10.3390/ijms22105262>.
- Chang, X., Cui, L., Hou, Y., Jensen, T.J., Aleksandrov, A.A., Mengos, A., Riordan, J.R., 1999. Removal of multiple arginine-framed trafficking signals overcomes misprocessing of $\Delta F508$ CFTR present in most patients with cystic fibrosis. *Mol. Cell.* 4, 137–142. [https://doi.org/10.1016/S1097-2765\(00\)80196-3](https://doi.org/10.1016/S1097-2765(00)80196-3).
- Costa, E., Girotti, S., Pauro, F., Leufkens, H.G.M., Cipolli, M., 2022. The impact of FDA and EMA regulatory decision - making process on the access to CFTR modulators for the treatment of cystic fibrosis. *Orphanet J. Rare Dis.* 17, 188. <https://doi.org/10.1186/s13023-022-02350-5>.
- da Silva, V.D., de Faria, B.M., Colombo, E., Ascari, L., Freitas, G.P.A., Flores, L.S., Cordeiro, Y., Romão, L., Buarque, C.D., 2019. Design, synthesis, structural characterization and in vitro evaluation of new 1,4-disubstituted-1,2,3-triazole derivatives against glioblastoma cells. *Bioorg. Chem.* 83, 87–97. <https://doi.org/10.1016/j.bioorg.2018.10.003>.
- da Silva, V.D., Silva, R.R., Gonçalves Neto, J., López-Corcuera, B., Guimarães, M.Z., Noël, F., Buarque, C.D., 2020. New α -Hydroxy-1,2,3-triazoles and 9H-Fluorenes-1,2,3-triazoles Synthesis and evaluation as Glycine transporter 1 inhibitors. *J. Brazilian Chem. Soc.* 31, 1258–1269. <https://doi.org/10.21577/0103-5053.20200011>.
- Daina, A., Michielin, O., Zoete, V., 2017. SwissADME: a free web tool to evaluate pharmacokinetics, drug-likeness and medicinal chemistry friendliness of small molecules. *Sci. Rep.* 7, 42717. <https://doi.org/10.1038/srep42717>.
- Dalemans, W., Barbry, P., Campigny, G., Jallat, S., Dott, K., Dreyer, D., Crustal, R.G., Pavirani, A., Lecocq, J.-P., Lazdunski, M., 1991. Altered chloride ion channel kinetics associated with the $\Delta F508$ cystic fibrosis mutation. *Nature* 354, 526–528. <https://doi.org/10.1038/354526a0>.
- Decarvalho, A.C.V., Gansheroff, L.J., Teem, J.L., 2002. Mutations in the nucleotide binding domain 1 signature motif region rescue processing and functional defects of cystic fibrosis transmembrane conductance regulator $\Delta F508$. *J. Biol. Chem.* 277, 35896–35905. <https://doi.org/10.1074/jbc.M205644200>.
- Dekkers, J.F., Berkens, G., Kruisselbrink, E., Vonk, A., Jonge, H.R. De, Janssens, H.M., Bronsveld, I., Graaf, E. Van De, Nieuwenhuis, E.E.S., Houwen, R.H.J., Vleggaar, F.P., Escher, J.C., Rijke, Y.B. De, Majoor, C.J., Heijerman, H.G.M., Groot, D.W. De, Clevers, H., Ent, Van Der, Beekman, J.M., 2016. Characterizing responses to CFTR-modulating drugs using rectal organoids derived from subjects with cystic fibrosis. *Sci. Transl. Med.* 8, 344ra84. <https://doi.org/10.1126/scitranslmed.aad8278>.
- Denning, G.M., Anderson, M.P., Amara, J.F., Marshall, J., Smith, A.E., Welsh, M.J., 1992. Processing of mutant cystic fibrosis transmembrane conductance regulator is temperature-sensitive. *Nature* 358, 761–764. <https://doi.org/10.1038/358761a0>.
- Fährrolfs, R., Bietz, S., Flachsenberg, F., Meyder, A., Nittinger, E., Otto, T., Volkamer, A., Rarey, M., 2017. ProteinsPlus: a web portal for structure analysis of macromolecules. *Nucleic Acids Res.* 45, W337–W343. <https://doi.org/10.1093/NAR/GKX333>.
- Farinha, C.M., King-Underwood, J., Sousa, M., Correia, A.R., Henriques, B.J., Roxo-Rosa, M., Da Paula, A.C., Williams, J., Hirst, S., Gomes, C.M., Amaral, M.D., 2013. Revertants, low temperature, and correctors reveal the mechanism of $\Delta F508$ -CFTR rescue by VX-809 and suggest multiple agents for full correction. *Chem. Biol.* 20, 943–955. <https://doi.org/10.1016/j.chembiol.2013.06.004>.
- Fiedorczuk, K., Chen, J., 2022. Mechanism of CFTR correction by type I folding correctors. *Cell* 185, 158–168. <https://doi.org/10.1016/j.cell.2021.12.009>.
- Gee, H.Y., Noh, S.H., Tang, B.L., Kim, K.H., Lee, M.G., 2011. Rescue of $\Delta F508$ -CFTR trafficking via a GRASP-dependent unconventional secretion pathway. *Cell* 146, 746–760. <https://doi.org/10.1016/j.cell.2011.07.021>.
- Hudson, R.P., Dawson, J.E., Chong, P.A., Yang, Z., Millen, L., Thomas, P.J., Brouillette, C. G., Forman-Kay, J.D., 2017. Direct binding of the corrector VX-809 to human CFTR NBD1: evidence of an allosteric coupling between the binding site and the NBD1:CL4 interface. *Mol. Pharmacol.* 92, 124–135. <https://doi.org/10.1124/mol.117.108373>.
- Jensen, T.J., Loo, M.A., Pind, S., Williams, D.B., Goldberg, A.L., Riordan, J.R., 1995. Multiple proteolytic systems, including the proteasome, contribute to CFTR processing. *Cell* 83, 129–135. [https://doi.org/10.1016/0092-8674\(95\)90241-4](https://doi.org/10.1016/0092-8674(95)90241-4).
- Kim, J., Noh, S.H., Piao, H., Kim, D.H., Kim, K., Cha, J.S., Chung, W.Y., Cho, H.S., Kim, J. Y., Lee, M.G., 2016. Monomerization and ER relocation of GRASP is a requisite for unconventional secretion of CFTR. *Traffic* 17, 733–753. <https://doi.org/10.1111/tra.12403>.
- Kim, S.J., Skach, W.R., 2012. Mechanisms of CFTR folding at the endoplasmic reticulum. *Front. Pharmacol.* 3, 201. <https://doi.org/10.3389/fphar.2012.00201>.
- Lewis, H.A., Buchanan, S.G., Burley, S.K., Connors, K., Dickey, M., Dorwart, M., Fowler, R., Gao, X., Guggino, W.B., Hendrickson, W.A., Hunt, J.F., Kearns, M.C., Lorimer, D., Maloney, P.C., Post, K.W., Rajashankar, K.R., Rutter, M.E., Sauder, J.M., Shriver, S., Thibodeau, P.H., Thomas, P.J., Zhang, M., Zhao, X., Emtage, S., 2004. Structure of nucleotide-binding domain 1 of the cystic fibrosis transmembrane conductance regulator. *EMBO J.* 23, 282–293. <https://doi.org/10.1038/sj.emboj.7600040>.
- Lipinski, C.A., 2004. Lead- and drug-like compounds: the rule-of-five revolution. *Drug Discov. Today Technol.* 1, 337–341. <https://doi.org/10.1016/j.ddtec.2004.11.007>.
- Liu, F., Zhang, Z., Levit, A., Levring, J., Touhara, K.K., Shoichet, B.K., Chen, J., 2019. Structural identification of a hotspot on CFTR for potentiation. *Science* 364, 1184–1188. <https://doi.org/10.1126/science.aaw7611>.
- Loo, T.W., Clarke, D.M., 2017. Corrector VX-809 promotes interactions between cytoplasmic loop one and the first nucleotide-binding domain of CFTR. *Biochem. Pharmacol.* 136, 24–31. <https://doi.org/10.1016/j.bcp.2017.03.020>.
- Lopes-Pacheco, M., 2020. CFTR modulators: the changing face of cystic fibrosis in the era of precision medicine. *Front. Pharmacol.* 10, 1662. <https://doi.org/10.3389/fphar.2019.01662>.
- Lopes-Pacheco, M., Bacalhau, M., Ramalho, S.S., Silva, I.A.L., Ferreira, F.C., Carlile, G. W., Thomas, D.Y., Farinha, C.M., Hanrahan, J.W., Amaral, M.D., 2022. Rescue of mutant CFTR trafficking defect by the investigational compound MCG1516A. *Cells* 11, 136. <https://doi.org/10.3390/cells11010136>.
- Lopes-Pacheco, M., Boinot, C., Sabirzhanova, I., Morales, M.M., Guggino, W.B., Cebotaru, L., 2015. Combination of correctors rescue $\Delta F508$ -CFTR by reducing its

- association with Hsp 40 and Hsp 27. *J. Biol. Chem.* 290, 25636–25645. <https://doi.org/10.1074/jbc.m115.671925>.
- Lopes-Pacheco, M., Boinot, C., Sabirzhanova, I., Rapino, D., Cebotaru, L.L., 2017. Combination of correctors rescues CFTR transmembrane-domain mutants by mitigating their interactions with proteostasis. *Cell. Physiol. Biochem.* 41, 2194–2210. <https://doi.org/10.1159/000475578>.
- Lopes-Pacheco, M., Pedemonte, N., Veit, G., 2021. Discovery of CFTR modulators for the treatment of cystic fibrosis. *Expet Opin. Drug Discov.* 16, 897–913. <https://doi.org/10.1080/17460441.2021.1912732>.
- Lopes-Pacheco, M., Sabirzhanova, I., Rapino, D., Morales, M.M., Guggino, W.B., Cebotaru, L., 2016. Correctors rescue CFTR mutations in nucleotide-binding domain 1 (NBD1) by modulating proteostasis. *ChemBiochem* 17, 493–505. <https://doi.org/10.1002/cbic.201500620>.
- Lopes-Pacheco, M., Silva, I.A.L., Turner, M.J., Carlile, G.W., Sondo, E., Thomas, D.Y., Pedemonte, N., Hanrahan, J.W., Amaral, M.D., 2020. Characterization of the mechanism of action of RDR01752, a novel corrector of F508del-CFTR. *Biochem. Pharmacol.* 180, 114133. <https://doi.org/10.1016/j.bcp.2020.114133>.
- Middleton, P.G., Mall, M.A., Dřevínek, P., Lands, L.C., McKone, E.F., Polineni, D., Ramsey, B.W., Taylor-Cousar, J.L., Tullis, E., Vermeulen, F., Marigowda, G., McKee, C.M., Moskowitz, S.M., Nair, N., Savage, J., Simard, C., Tian, S., Waltz, D., Xuan, F., Rowe, S.M., Jain, R., 2019. Elexacaftor–Tezacaftor–Ivacaftor for Cystic Fibrosis with a Single Phe508del Allele. *N. Engl. J. Med.* 381, 1809–1819. <https://doi.org/10.1056/nejmoa1908639>.
- Pedemonte, N., Lukacs, G.L., Du, K., Caci, E., Zegarar-Moran, O., Galletta, L.J.V., Verkman, A.S., 2005. Small-molecule correctors of defective Δ F508-CFTR cellular processing identified by high-throughput screening. *J. Clin. Invest.* 115, 2564–2571. <https://doi.org/10.1172/JCI24898>.
- Pedemonte, N., Tomati, V., Sondo, E., Galletta, L.J.V., 2010. Influence of cell background on pharmacological rescue of mutant CFTR. *Am. J. Physiol. Cell Physiol.* 298, C866–C874. <https://doi.org/10.1152/ajpcell.00404.2009>.
- Pinto, M.C., Silva, I.A.L., Figueira, M.F., Amaral, M.D., Lopes-Pacheco, M., 2021. Pharmacological modulation of ion channels for the treatment of cystic fibrosis. *J. Exp. Pharmacol.* 13, 693–723. <https://doi.org/10.2147/JEP.S255377>.
- Prins, S., Corradi, V., Sheppard, D.N., Tieleman, D.P., Vergani, P., 2022. Can two wrongs make a right? F508del-CFTR ion channel rescue by second-site mutations in its transmembrane domains. *J. Biol. Chem.* 298, 101615. <https://doi.org/10.1016/j.jbc.2022.101615>.
- Rabeh, W.M., Bossard, F., Xu, H., Oliyoned, T., Bagdany, M., Mulvihill, C.M., Du, K., de Bernado, S., Liu, Y., Konermann, L., Roldan, A., Lukacs, G.L., 2012. Correction of both NBD1 energetics and domain interface is required to restore Δ F508 CFTR folding and function. *Cell* 148, 150–163. <https://doi.org/10.1016/j.cell.2011.11.024>.
- Ramallo, S.S., Silva, I.A.L., Amaral, M.D., Farinha, C.M., 2022. Rare trafficking cfr mutations involve distinct cellular retention machineries and require different rescuing strategies. *Int. J. Mol. Sci.* 23, 24. <https://doi.org/10.3390/ijms23010024>.
- Rapino, D., Sabirzhanova, I., Lopes-Pacheco, M., Grover, R., Guggino, W.B., Cebotaru, L., 2015. Rescue of NBD2 mutants N1303K and S1235R of CFTR by small-molecule correctors and transcomplementation. *PLoS One* 10, e0119796. <https://doi.org/10.1371/journal.pone.0119796>.
- Ren, H.Y., Grove, D.E., De La Rosa, O., Houck, S.A., Sopha, P., Van Goor, F., Hoffman, B. J., Cyr, D.M., 2013. VX-809 corrects folding defects in cystic fibrosis transmembrane conductance regulator protein through action on membrane-spanning domain 1. *Mol. Biol. Cell* 24, 3016–3024. <https://doi.org/10.1091/mbc.E13-05-0240>.
- Riordan, J.R., Rommens, J.M., Kerem, B.S., Alon, N.O.A., Rozmahel, R., Grzelczak, Z., Zielenski, J., Lok, S.I., Plavski, N., Chou, J.L., Drumm, M.L., Iannuzzi, M.C., Collins, F.S., Tsui, L.C., 1989. Identification of the cystic fibrosis gene: Cloning and characterization of complementary DNA. *Science* 245, 1066–1073. <https://doi.org/10.1126/science.2475911>.
- Roxo-Rosa, M., Xu, Z., Schmidt, A., Neto, M., Cai, Z., Soares, C.M., Sheppard, D.H., Amaral, M.D., 2006. Revertant mutants G550E and 4Rk rescue cystic fibrosis mutants in the first nucleotide-binding domain of CFTR by different mechanisms. *Proc. Natl. Acad. Sci. U.S.A.* 103, 17891–17896. <https://doi.org/10.1073/pnas.0608312103>.
- Roy, G., Chalfin, E.M., Saxena, A., Wang, X., 2010. Interplay between ER exit code and domain conformation in CFTR misprocessing and rescue. *Mol. Biol. Cell* 21, 597–609. <https://doi.org/10.1091/mbc.e09-05-0427>.
- Schöning-Stierand, K., Diedrich, K., Fährrolfs, R., Flachsenberg, F., Meyder, A., Nittinger, E., Steinegger, R., Rarey, M., 2020. ProteinsPlus: interactive analysis of protein–ligand binding interfaces. *Nucleic Acids Res.* 48, W48. <https://doi.org/10.1093/NAR/GKAA235>. –W53.
- Sharma, M., Benharouga, M., Hu, W., Lukacs, G.L., 2001. Conformational and temperature-sensitive stability defects of the Δ F508 cystic fibrosis transmembrane conductance regulator in post-endoplasmic reticulum compartments. *J. Biol. Chem.* 276, 8942–8950. <https://doi.org/10.1074/jbc.M009172200>.
- Sheppard, D.N., Rich, D.P., Ostedgaard, L.S., Gregory, R.J., Smith, A.E., Welsh, M.J., 1993. Mutations in CFTR associated with mild-disease-form CI- channels with altered pore properties. *Nature* 362, 160–164. <https://doi.org/10.1038/362160a0>.
- Silva, I.A.L., Laselva, O., Lopes-Pacheco, M., 2022. Advances in preclinical in vitro models for the translation of precision medicine for cystic fibrosis. *J. Personalized Med.* 12, 1321. <https://doi.org/10.3390/jpm12081321>.
- Silva, I.A.L., Railean, V., Duarte, A., Amaral, M.D., 2021. Personalized medicine based on nasal epithelial cells: comparative studies with rectal biopsies and intestinal organoids. *J. Personalized Med.* 11, 421. <https://doi.org/10.3390/jpm11050421>.
- Singh, A.K., Fan, Y., Balut, C., Alani, S., Manelli, A.M., Swensen, A.M., Jia, Y., Neelands, T.R., Vortherms, T.A., Liu, B., Searle, X.B., Wang, X., Gao, W., Hwang, T. C., Ren, H.Y., Cyr, D., Kym, P.R., Conrath, K., Tse, C., 2020. Biological characterization of F508delCFTR protein processing by the CFTR corrector ABBV-2222/GLPG2222. *J. Pharmacol. Exp. Therapeut.* 372, 107–118. <https://doi.org/10.1124/jpet.119.261800>.
- Sondo, E., Tomati, V., Caci, E., Esposito, A.I., Pfeffer, U., Pedemonte, N., Galletta, L.J.V., 2011. Rescue of the mutant CFTR chloride channel by pharmacological correctors and low temperature analyzed by gene expression profiling. *Am. J. Physiol. Cell Physiol.* 301, C872–C885. <https://doi.org/10.1152/ajpcell.00507.2010>.
- Sutharsan, S., McKone, E.F., Downey, D.G., Duckers, J., MacGregor, G., Tullis, E., Van Braeckel, E., Wainwright, C.E., Watson, D., Ahluwalia, N., Bruinsma, B.G., Harris, C., Lam, A.P., Lou, Y., Moskowitz, S.M., Tian, S., Yuan, J., Waltz, D., Mall, M.A., 2022. Efficacy and safety of elexacaftor plus tezacaftor plus ivacaftor versus tezacaftor plus ivacaftor in people with cystic fibrosis homozygous for F508del-CFTR: a 24-week, multicentre, randomised, double-blind, active-controlled, phase 3b trial. *Lancet Respir. Med.* 10, 267–277. [https://doi.org/10.1016/S2213-2600\(21\)00454-9](https://doi.org/10.1016/S2213-2600(21)00454-9).
- Thibodeau, P.H., Richardson 3rd, J.M., Wang, W., Millen, L., Watson, J., Mendoza, J.L., Du, K., Fischman, S., Senderowitz, H., Lukacs, G.L., Kirk, K., Thomas, P.J., 2010. The cystic fibrosis-causing mutation Δ F508 affects multiple steps in cystic fibrosis transmembrane conductance regulator biogenesis. *J. Biol. Chem.* 285, 35825–35835. <https://doi.org/10.1074/jbc.M110.131623>.
- Thomsen, R., Christensen, M.H., 2006. MolDock: a new technique for high-accuracy molecular docking. *J. Med. Chem.* 49, 3315–3321. <https://doi.org/10.1021/jm051197e>.
- Van Goor, F., Straley, K.S., Cao, D., González, J., Hadida, S., Hazlewood, A., Joubran, J., Knapp, T., Makings, L.R., Miller, M., Neuberger, T., Olson, E., Panchenko, V., Rader, J., Singh, A., Stack, J.H., Tung, R., Grootenhuys, P.D.J., Negulescu, P., 2006. Rescue of Δ F508-CFTR trafficking and gating in human cystic fibrosis airway primary cultures by small molecules. *Am. J. Physiol. Lung Cell Mol. Physiol.* 290, L1117–L1130. <https://doi.org/10.1152/ajplung.00169.2005>.
- Van Goor, F., Yu, H., Burton, B., Hoffman, B.J., 2014. Effect of ivacaftor on CFTR forms with missense mutations associated with defects in protein processing or function. *J. Cyst. Fibros.* 13, 29–36. <https://doi.org/10.1016/j.jcf.2013.06.008>.
- Veit, G., Roldan, A., Hancock, M.A., da Fonte, D.F., Xu, H., Hussein, M., Frenkiel, S., Matouk, E., Velkov, T., Lukacs, G.L., 2020. Allosteric folding correction of F508del and rare CFTR mutants by elexacaftor-tezacaftor-ivacaftor (Trikafta) combination. *JCI Insight* 5, e139983. <https://doi.org/10.1172/JCI.INSIGHT.139983>.
- Veit, G., Velkov, T., Xu, H., Vadeboncoeur, N., Bilodeau, L., Matouk, E., Lukacs, G.L., 2021. A precision medicine approach to optimize modulator therapy for rare cfr folding mutants. *J. Personalized Med.* 11, 643. <https://doi.org/10.3390/jpm11070643>.
- Veit, G., Xu, H., Dreano, E., Avramescu, R.G., Bagdany, M., Beitel, L.K., Roldan, A., Hancock, M.A., Lay, C., Li, W., Morin, K., Gao, S., Mak, P.A., Ainscow, E., Orth, A.P., McNamara, P., Edelman, A., Frenkiel, S., Matouk, E., Sermet-Gaudelus, I., Barnes, W. G., Lukacs, G.L., 2018. Structure-guided combination therapy to potentially improve the function of mutant CFTRs. *Nat. Med.* 24, 1732–1742. <https://doi.org/10.1038/s41591-018-0200-x>.
- Volkamer, A., Griewel, A., Grombacher, T., Rarey, M., 2010. Analyzing the topology of active sites: on the prediction of pockets and subpockets. *J. Chem. Inf. Model.* 50, 2041–2052. <https://doi.org/10.1021/C100241Y>.
- Volkamer, A., Kuhn, D., Grombacher, T., Rippmann, F., Rarey, M., 2012. Combining global and local measures for structure-based druggability predictions. *J. Chem. Inf. Model.* 52, 360–372. <https://doi.org/10.1021/C1200454V>.
- Wang, X., Huang, B., Liu, X., Zhan, P., 2016. Discovery of bioactive molecules from CuAAC click-chemistry-based combinatorial libraries. *Drug Discov. Today* 21, 118–132. <https://doi.org/10.1016/j.drudis.2015.08.004>.
- Wang, X., Koulov, A.V., Kellner, W.A., Riordan, J.R., Balch, W.E., 2008. Chemical and biological folding contribute to temperature sensitive Δ F508 CFTR Trafficking.pdf. *Traffic* 9, 1878–1893. <https://doi.org/10.1111/j.1600-0854.2008.00806.x>.
- Wang, X., Matteson, J., An, Y., Moyer, B., Yoo, J., Bannykh, S., Wilson, I.A., Riordan, J. R., Balch, W.E., 2004. COPII-dependent export of cystic fibrosis transmembrane conductance regulator from the ER uses a di-acidic exit code. *J. Cell Biol.* 167, 65–74. <https://doi.org/10.1083/jcb.200401035>.
- Zhang, D., Cicciello, F., Anjos, S.M., Carissimo, A., Liao, J., Carlile, G.W., Balghi, H., Robert, R., Luini, A., Hanrahan, J.W., Thomas, D.Y., 2012. Ouabain mimics low temperature rescue of F508del-CFTR in cystic fibrosis epithelial cells. *Front. Pharmacol.* 3, 176. <https://doi.org/10.3389/fphar.2012.00176>.